Phytoplankton biodiversity is more important for ecosystem functioning in highly variable thermal environments

Elvire Bestion, Bart Haegeman, Soraya Alvarez Codesal, Alexandre Garreau, Michèle Huet, Samuel Barton, José M Montoya

Phytoplankton biodiversity is more important for ecosystem functioning in highly variable thermal environments

Elvire Bestion[1*], Bart Haegeman[1], Soraya Alvarez Codesal[1], Alexandre Garreau[1], Michèle Huet[1], Samuel Barton[2,3], José M. Montoya[1]

Proceedings of the National Academy of Sciences, 2021, doi : 10.1073/pnas.2019591118

[1]Station d'Ecologie Théorique et Expérimentale, CNRS, Moulis, 09200, France
[2]Environment and Sustainability Institute, University of Exeter, Penryn Campus, Penryn, Cornwall, TR10 9FE UK
[3]Department of Earth Sciences, University of Oxford, Oxford OX1 3AN, UK
ORCID ID: 0000-0001-5622-7907 (EB), 0000-0003-2325-4727 (BH), 0000-0001-6399-1954 (SAC), 0000-0003-3094-6174 (MH), 0000-0003-2551-4297 (SB), 0000-0002-6676-7592 (JMM)
** Correspondence to: e.bestion@outlook.com*

Abstract

The twenty-first century has seen an acceleration of anthropogenic climate change and biodiversity loss, with both stressors deemed to affect ecosystem functioning. However, we know little about the interactive effects of both stressors, and in particular about the interaction of increased climatic variability and biodiversity loss on ecosystem functioning. This should be remedied because larger climatic variability is one of the main features of climate change. Here we demonstrated that temperature fluctuations led to changes in the importance of biodiversity for ecosystem functioning. We used microcosm communities of different phytoplankton species richness and exposed them to a constant, mild and severe temperature fluctuating environment. Wider temperature fluctuations led to steeper biodiversity-ecosystem functioning slopes, meaning that species loss had a stronger negative effect on ecosystem functioning in more fluctuating environments. For severe temperature fluctuations, the slope increased through time due to a decrease of the productivity of species-poor communities over time. We developed a theoretical competition model to better understand our experimental results, and showed that larger differences in thermal tolerances across species led to steeper biodiversity-ecosystem functioning slopes. Species-rich communities maintained their ecosystem functioning with increased fluctuation as they contained species able to resist the thermally fluctuating environments, while this was on average not the case in species-poor communities. Our results highlight the importance of biodiversity for maintaining ecosystem functions and services in the context of increased climatic variability under climate change.

Significance statement

The combined acceleration of climate change and biodiversity loss necessitates understanding how ecosystem functions and services will be affected. Most studies focus on the effects of increasing mean temperatures, but climate change will increase temperature fluctuations too. We performed an experiment and developed a model to understand how increased temperature fluctuations affected the importance of biodiversity for ecosystem functioning in phytoplankton communities. Increased temperature fluctuations led to steeper biodiversity-ecosystem functioning slopes, which indicates that biodiversity loss has a stronger negative effect on ecosystem functioning than when conditions are more stable. Our model suggests that steeper slopes are associated with variation in thermal tolerances across species, as species-rich systems contained species able to resist the thermally fluctuating environments.

Keywords: Climate change, climate variability, temperature fluctuations, biodiversity loss, marine phytoplankton, biodiversity-ecosystem functioning, thermal tolerance

Introduction

Climate change and biodiversity loss are two of the most pressing ecological issues of the century (1, 2). Because biodiversity is positively related to ecosystem functioning (3–8), the accelerating species loss is expected to lead to a decrease in ecosystem functioning and ecosystem services (9–13).

Climate change increases both the mean and variance in temperature (1, 14), which can further hamper ecosystem functioning (15–17). Increased temperature variance in particular is expected to pose a greater risk to biodiversity than increased mean (18, 19). However, much less is known about the potential interactive effects of biodiversity loss and climate change on ecosystem functioning (but see (20–23)), and particularly between the potential interactive effects of biodiversity loss and temperature fluctuations. To better understand the potential impacts of increased climatic variation and biodiversity loss on ecosystems, it is thus important to investigate the effect of temperature fluctuations on the biodiversity-ecosystem functioning relationship.

Climate change has complex effects on biodiversity and ecosystem functioning. Warmer climates can lead to both a loss (24–29) and an increase in biodiversity (30, 31). At the local scale, the effect of increased temperature on species richness shows mixed trends, with studies finding declines (32–34), increases (30, 35) or no discernible trend (36, 37). The effects of increased thermal variability also remain unclear, positive, negative or no effects on richness have been reported (16, 38–42). Further, climate change can alter ecosystem functioning, either directly or indirectly through changes in biodiversity (16, 43–47).

In addition to affecting diversity and ecosystem functioning, increased temperature mean and variation can modify the relationship between biodiversity and ecosystem functioning. In bacteria and phytoplankton, warmer temperatures resulted in a steeper slope of the relationship between log ecosystem functioning and log species richness (21, 22, 48). Steeper slopes of the biodiversity-ecosystem functioning relationship indicate that the effect of biodiversity on ecosystem functioning is stronger in warmer environments, i.e., the loss of one species has a more detrimental effect on ecosystem functioning as temperatures increase. Interestingly, a recent study on picophytoplankton showed that the steepness of the biodiversity-ecosystem functioning slope relied on both short-term temperature and community evolutionary history (23). Less is known about the effect of temperature fluctuations on biodiversity-ecosystem functioning relationships. A study on a protozoan-bacteria consumer resource relationships showed that the slope between diversity and biomass became shallower with increased fluctuations (49); another study on fungal assemblages showed that polycultures decomposed leaves better than monocultures under fluctuating temperatures (50).

Several mechanisms might lead to a change in the relationship between biodiversity and ecosystem functioning with temperature fluctuations. We focus on three mechanisms of potential relevance on fluctuating environments: tolerance differences, species interactions and temporal asynchrony. Firstly, different species within a community have different thermal tolerances, i.e., they handle thermal stress differently. When temperature mean or fluctuation increases, these underlying interspecific differences can manifest more strongly. This, in turn, can lead species-rich communities to perform better than species-poor communities due to their containing of species able to resist the stressful conditions, leading to increased slopes of biodiversity-ecosystem functioning with stress (51). This was the case in marine phytoplankton communities, where differences in species thermal tolerances led to a larger effect of biodiversity on ecosystem functioning in more physiologically stressful, warmer environments (22). Theory suggests that when the environment becomes too stressful and exceeds the thermal tolerances of all species, the slopes of biodiversity-ecosystem functioning (BEF) become shallower again (48, 51). In a context of increased temperature fluctuations, one can expect that differences in average tolerances to the varying environmental conditions among species would lead to variation in the relationship of ecosystem functioning with species richness. Thus, we expect that communities with a larger spread in thermal tolerances should have a steeper biodiversity-ecosystem functioning relationship.

Secondly, species interactions can change in response to changes in the thermal environment. Strong competition among species can lead to shallower biodiversity-ecosystem functioning slopes, where adding one species does not increase ecosystem functioning much when species compete for the same resources (i.e., small niche differences (52, 53)). On the contrary, large niche differences or facilitative interactions can lead to opposite relationships, where adding one species strongly increases overall ecosystem functioning. If increased temperature fluctuations cause a change in competitive interactions, this in turn can lead to a modification of the BEF slope. Models investigating the effect of temperature mean and variation on BEF relationships have suggested that temperature-driven changes in the intensity of competition could indeed play a role in driving the relationship (49).

Thirdly, asynchrony in species temporal dynamics within a community, for instance due to temperature fluctuations, can lead to increased ecosystem productivity and temporal stability through an insurance effect (5, 54). This can lead to a community that is dominated by different species depending on their tolerance to the current environmental conditions (e.g. "warm-adapted" species increasing in abundance and dominating when temperature is hotter, and "cold-adapted" species dominating when temperature is cooler). Such mechanism would lead more diverse communities to perform better in thermally fluctuating environments than species-poor communities. These three mechanisms can co-occur and lead to changes in biodiversity-ecosystem functioning with temperature fluctuations.

The effects of biodiversity on ecosystem functioning often increases through time (55, 56). Thus, the impact of species loss on functioning is larger as ecosystems assemble. Such temporal effects can arise from a temporal increase in productivity of species-rich communities (e.g. through increases in complementarity through time, for instance when legumes increase nutrient availability for other plant species by fixing atmospheric nitrogen), a decrease in productivity of species-poor communities (e.g. through increases in abundance of antagonistic soil microorganisms in plant communities), or a combination of both (55, 57, 58). Temporal fluctuations could, in turn, interfere with ecosystem temporal dynamics, and it is worth investigating whether this could lead to changes in the biodiversity-ecosystem relationships over time.

Here we used a proof-of-concept experiment and a theoretical model to understand how increasing temperature fluctuations affected biodiversity-ecosystem functioning relationships, and whether these relationships changed over time. We experimentally manipulated the species richness of phytoplankton communities at a control temperature of 25°C, a moderate temperature fluctuation treatment of between 22 and 28°C every other day, and a severe fluctuation treatment of between 19 and 31°C every other day using a random partitioning experimental design ((59), Fig. 1). We quantified the impact of temperature fluctuations and temporal scale (i.e., after 5 and 15 days) on the relationship between biodiversity and ecosystem production. This experimental design allowed quantifying the impacts of random species loss on ecosystem functioning as well as evaluating the relative contribution of each species to ecosystem production. We used three measures of ecosystem production, either total cell abundance, total biomass or total chlorophyll *a* content. Such measures have been used in similar experiments (22, 48, 49), and measures of biomass production have been widely used in plants (11). However, it is to note that ecosystem functioning can be also measured as a flux, such as C fixation, O_2 production or nutrient recycling, that we were unfortunately unable to measure here. Including such fluxes could lead to different expectations of the BEF slope, and is beyond the scope of our study. We further explored the relative importance of the three different mechanisms outlined above (tolerance differences, species interactions and temporal asynchrony) as drivers of our experimental results. We did so by means of our experimental data and a simple theoretical model of species competition. In particular, we tested whether potential changes in biodiversity-ecosystem function slope were linked to a change in species interactions or a greater spread in thermal tolerances, and explored the impact of temporal asynchrony in the model, using cell abundance as a measure for ecosystem function.

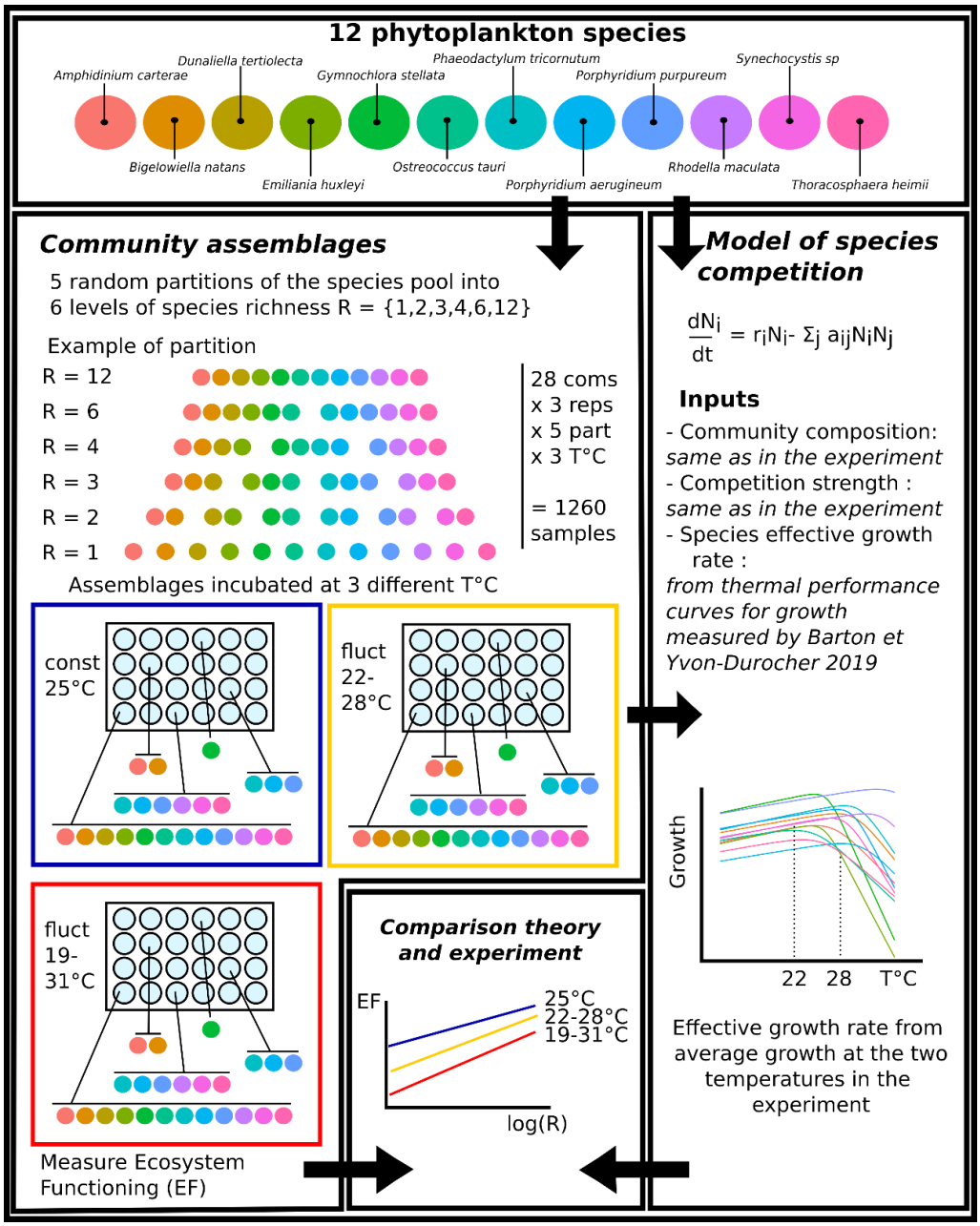

Fig. 1: Flow chart of the experimental design and its comparison with the theoretical model

Results

Biodiversity-ecosystem functioning relationships across time and temperature fluctuation regimes

Ecosystem production measured as phytoplankton cell abundance increased linearly with species richness on a log-log scale, corresponding to a power-law dependence on linear scales. The slope of the relationship between biodiversity and ecosystem functioning (BEF), which quantifies the effect of the loss of one species on ecosystem functioning, varied with temperature fluctuation treatment and with time, with a triple interaction between richness, temperature fluctuations and time of sampling (Fig. 2, Table 1). A contrast analysis showed no statistically significant differences in the slopes of BEF

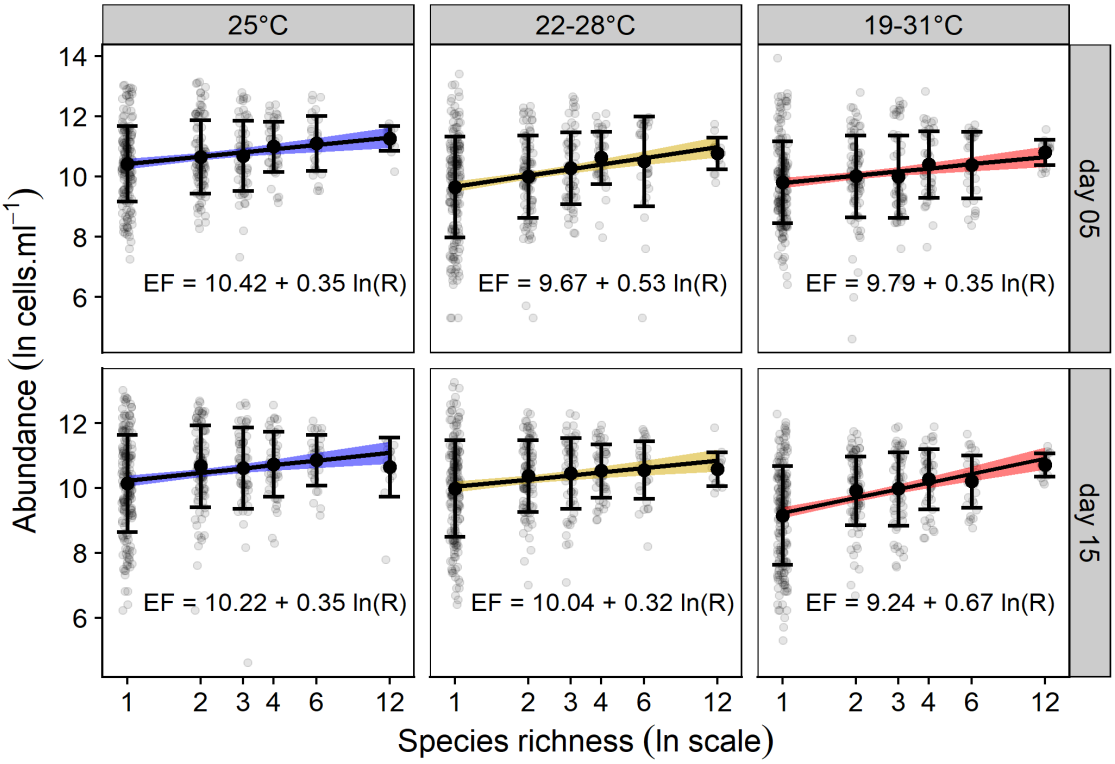

Fig. 2: The relationship between biodiversity and ecosystem functioning depends on the interaction between temperature fluctuation treatment and time.
From left to right: constant 25°C temperature treatment (blue confidence interval), alternating 22 and 28°C temperature every other day (yellow confidence interval), and alternating 19 and 31°C temperature every other day (red confidence interval). Top panel: 5 days, and bottom panel: 15 days of experiment. Grey points represent ecosystem functioning for each of the 1260 communities (420 per temperature fluctuation treatment) measured as ln total cell abundance (ln cells.ml^{-1}). Black points and error bars are the mean ± SD for each level of species richness. Lines and confidence intervals correspond to the fitted curves for the most parsimonious linear mixed model (Table 1). The slope of the relationship between biodiversity and ecosystem functioning depends on the interaction between temperature treatment and time (Table 1), with no differences in slopes between treatments after 5 days but an increase in the slope of the extreme fluctuation treatment over time leading to steeper BEF slopes at high levels of temperature fluctuations at the end of the experiment (Table S1).

relationships between temperature fluctuation treatments after 5 days (Fig. 2, Table S1). However, by the end of the experiment (after 15 days), the slope increased for the moderate and extreme temperature fluctuation treatment, leading to steeper BEF slopes for larger temperature fluctuations (Fig. 2, Table S1). This meant that when thermal fluctuation was large, the loss of a species had a stronger negative effect on total community abundance than in environments that were less variable. At constant temperatures, the exponent of the relationship between cell abundance and species richness at day 15 on a log-log scale was 0.35 ± 0.09, while it was twice this value in the severe fluctuation treatment, at 0.67 ± 0.09 (Fig. 2).

The intercepts of the BEF relationships, which represent the mean ecosystem functioning when species richness was equal to one, also varied among treatments. We found a higher total community abundance in the constant relative to the two fluctuating treatments after 5 days, and in the constant and mildly fluctuating relative to the severely fluctuating treatment after 15 days (Fig. 2-3, Table S2). Interestingly, the greater BEF slope compensated almost

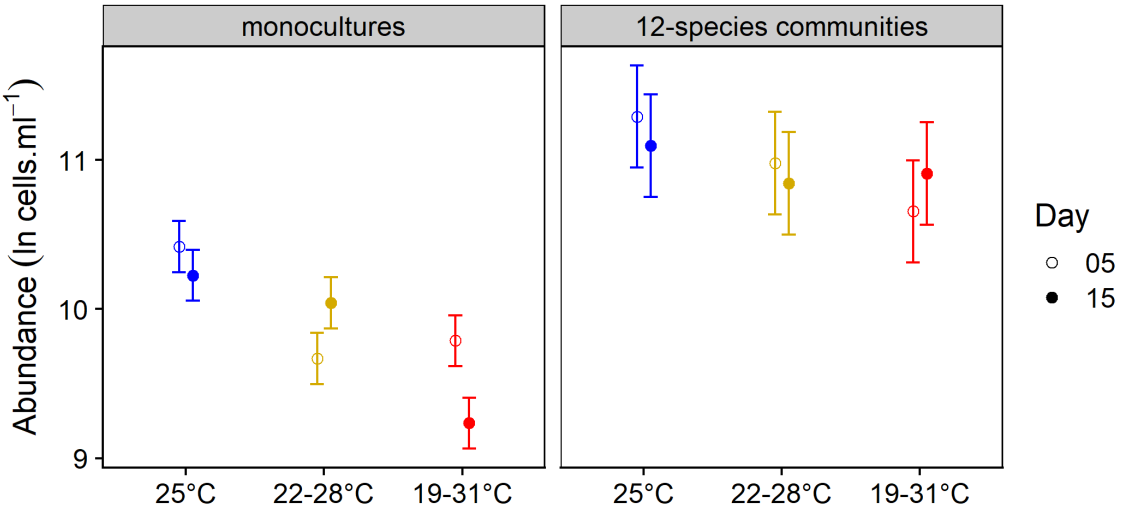

Fig. 3: Comparing ecosystem functioning for the monocultures and 12-species communities across the different temperature fluctuation treatments.
Values of ecosystem functioning (abundance in ln cells.ml^{-1}) for the monocultures and 12-species communities in the three temperature fluctuation treatments and the two times. Values and 95% confidence intervals are derived from a contrast analysis of the model represented in Fig. 2 (Table S2). Increased temperature fluctuations lead to lower ecosystem functioning in the low richness communities, while this detrimental effect is compensated for the 12-species rich communities (Table S2). Further, increased temperature fluctuations lead to decreased ecosystem functioning over time in the low richness communities (Table S3), with no effect in the species rich communities.

completely for this negative effect of thermal fluctuations on total community abundance for the richest communities (i.e., those initiated with 12 species), with a slightly lower total community abundance in the severely fluctuating treatment compared to the constant environment after 5 days, and no differences after 15 days (Fig. 3, Table S2). Further, temporal effects at the severe fluctuation treatment were linked to a decrease in total community abundance over time for the low richness communities, with no change for the high richness communities (Fig. 3, Table S3).

When using both total biomass and total chlorophyll *a* as measures of ecosystem production, we found similar results as for abundance, with a triple interaction between time, biodiversity and temperature fluctuation treatment on ecosystem function (Fig. S1-S2, Table S4-S7). A contrast analysis of the high- and low-richness communities showed that for low-richness communities, the severely fluctuating treatment had lower values of total chlorophyll *a* than the two other treatments at both temporal scales, and this negative effect was compensated for the most diverse communities, with no difference between temperature treatments (Fig. S3, Table S8). Finally, temporal increases in BEF slope for chlorophyll *a* were linked to a steeper increase in ecosystem functioning with time for the high-richness compared to the low-richness communities (Fig. S3, Table S9). When using biomass as a measure, we found similar results, with lower values of total biomass across time in the severely fluctuating treatment in the low richness communities, while this negative effect was compensated after 15 days for the high richness communities (Table S10-S11, Fig S4).

Exploration of the mechanisms

We investigated both theoretically and empirically the mechanisms related to the observed changes in biodiversity-ecosystem functioning slopes with ecosystem functioning

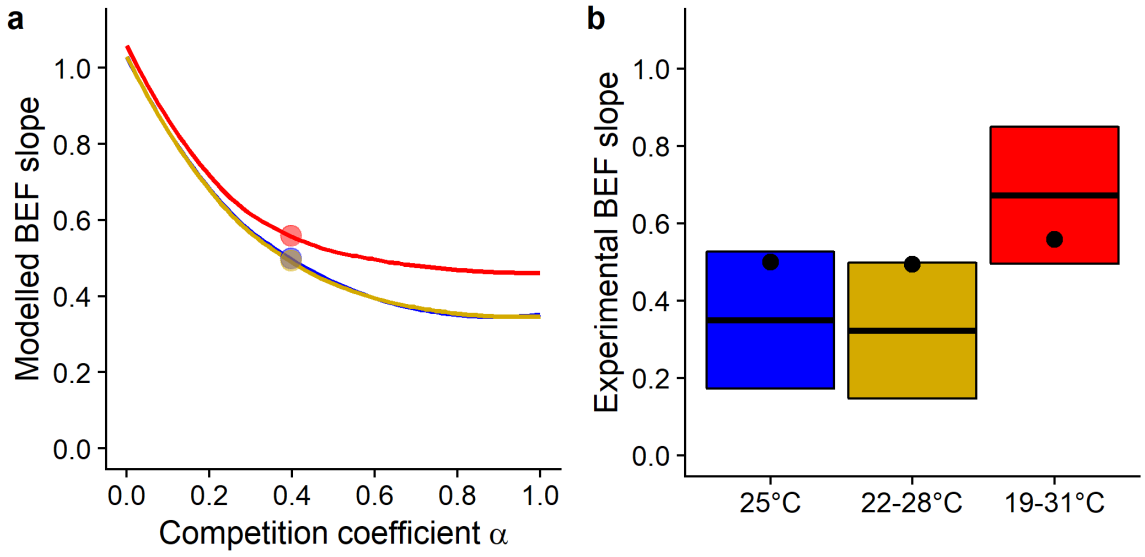

Fig. 4: Comparison of the modelled and experimental results regarding the slope of the biodiversity-ecosystem functioning relationship.
a) Modelled BEF slope depending on the temperature (blue: constant 25°C treatment, yellow: fluctuating 22-28°C treatment, and red: fluctuating 19-31°C treatment) and on the competition coefficient α (see Fig. S6). The dots correspond to the competition coefficient estimated in our experiment (see Fig. S7). b) Experimental BEF slopes at day 15 in the three temperature treatments compared to the modelled slopes. Boxplots correspond to effect sizes and 95% CI, and dots to the modelled BEF slopes for α equal to the observed 0.40 value (Fig. S6).

measured as community abundance. We created a simple competition model parametrized with species thermal tolerances (Fig S5), in which the competition coefficient between species α could vary. We first showed that severely fluctuating temperature treatments led overall to steeper BEF slopes than constant or mild thermal fluctuation treatments (Fig. 4a). When we parametrized our model with both the species thermal tolerances and the competition coefficient derived from the experimental data (Fig. S6), the theoretical outcomes fell within the 95% confidence intervals of the experimental slopes (Fig. 4b, Fig. S7). Further, comparing the modelled ecosystem functioning values among treatments for the monocultures and the 12-species communities, we found similar patterns as for the experimental data: severe fluctuations leading to lower ecosystem functioning in low-richness communities, an effect nullified in the high-richness communities (Fig. S8).

A first mechanism potentially driving the observed change in the BEF slope is a change in the spread in species thermal tolerances. In our experiment, species differed in their thermal tolerances, and showed a wider spread in the distribution of tolerance to thermal fluctuations in the severe fluctuation compared to mild fluctuation and constant temperature treatments (Fig. S5). A theoretical exploration of our model shows that a wider spread in thermal tolerances can lead to steeper BEF slopes (Appendix 1, Fig. S9). Indeed, when conditions are good, such as at 25°C, all species are able to perform relatively well, and adding new species will lead to a small increase in ecosystem functioning. However, when the conditions become more stressful, such as in the 19-31°C fluctuation treatment, only a handful of species are able to tolerate these new conditions. Thus increasing the biodiversity leads to a greater chance that the community will contain at least one species able to tolerate the conditions, with a strong increase of ecosystem functioning with biodiversity. We further explored the effect of this spread on the experimental data. If spread is important in driving changes in BEF relationships, we expect that there should be an interactive effect of species richness and spread in thermal

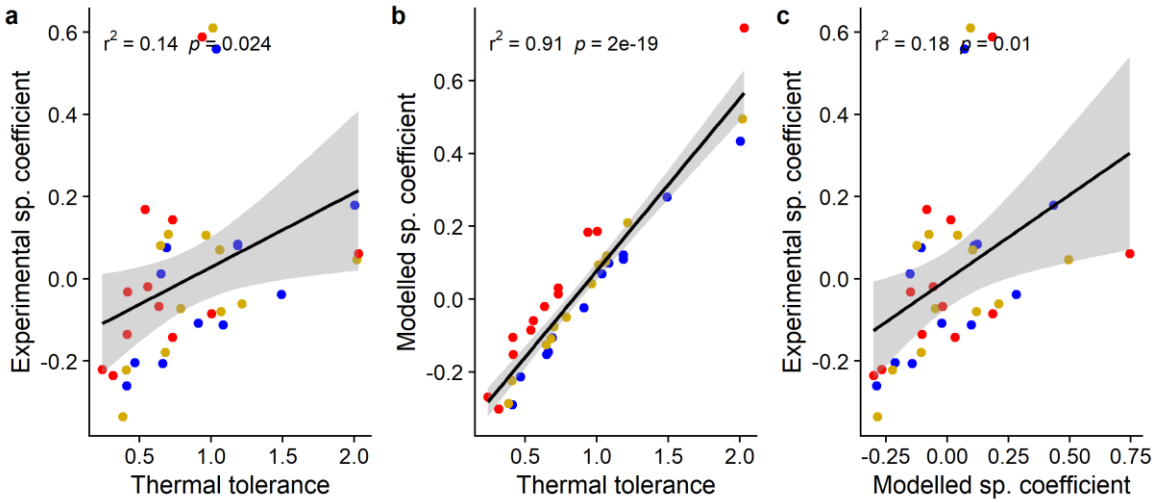

Fig. 5: Species contribution to ecosystem functioning depends on their thermal tolerance.

a) Relationship between species contribution to ecosystem functioning (species coefficient, Fig. S10) measured in the experiment and thermal tolerance measured as the mean growth over the three temperature fluctuation treatments from thermal tolerance curves (effective growth rate, Fig. S5). b) Relationship between species contribution to ecosystem functioning derived from the theoretical data and thermal tolerance. c) Relationship between species contribution to ecosystem functioning in the experiment and contribution to ecosystem functioning derived from the model results. Blue: constant 25°C treatment, yellow: fluctuating 22-28°C treatment, red: fluctuating 19-31°C treatment. N = 36 (12 species per temperature treatment).

tolerances of the species pool on ecosystem functioning. In particular, BEF slopes should be steeper for wider spread of thermal tolerances in the species pool, and species with a greater thermal tolerance would contribute more to ecosystem functioning. Our experimental results agree with both expectations: we found that the relative spread in effective growth rate within the species pool interacted with species richness to drive ecosystem function measured as total abundance (value for the interaction: $F_{1,1256} = 9.1$, $p = 0.003$, $R^2 = 0.12$). Alternative measures of spread, such as the coefficient of variation of thermal tolerances, gave the same significant interaction ($F_{1,1256} = 9.4$, $p = 0.002$, $R^2 = 0.12$). Further, the species that had the highest effective growth rate (i.e., average of growth rate at the two extreme temperatures of the treatment from a thermal tolerance curve ((60), Fig. S5)) had the largest contribution to ecosystem functioning measured as total abundance, as shown by the positive relationship between species coefficient (a measure of contribution to ecosystem functioning (59), where positive and negative values indicate an above- and below-average contribution to ecosystem functioning respectively, Fig. S10) and thermal tolerance (Fig. 5a). Further, we found the same relationship between modelled species coefficient and thermal tolerance (Fig. 5b), and a correlation between experimental and theoretically derived species coefficients (Fig. 5c). It is interesting to note that our results might be driven by the choice of species, as the larger spread of thermal tolerances in the 19-31°C fluctuating treatment is largely due to the high tolerance of *Ostreococcus tauri* (Fig. S5). Redoing model simulations without this species yielded a strong decrease in the difference in B-EF slope between treatments, although the slope was still steeper in the severely fluctuating treatment (Fig. S11). Part of the effect of biodiversity on ecosystem functioning is due to idiosyncratic effects of the species composition, as shown by the effect of species identity (Fig. 5). Results might vary quantitatively with different species pools, but the slope of the BEF relationship should be steeper in severely fluctuating treatments as the chance to find a species that is highly tolerant

Table 1. Comparison of linear mixed models estimating the effect of temperature fluctuations, species richness and time on ecosystem production.

The linear mixed models describe the effect of temperature fluctuations (T, as a factor), species richness (ln(R)), time (D, days since the start of the experiment, as a factor) and their interaction, plus a random effect of sample identity on ecosystem functioning. At each step, terms are added to the linear model and we compare the two models through a likelihood ratio test. Marginal and conditional R^2 and AIC are calculated for each model, as well as ΔAIC from the model with lowest AIC and AIC weights. Lower AIC values indicate an improved model. Analyses revealed that the model with lowest AIC included the interaction between temperature fluctuations, time and species richness. See Table S1 for a post hoc, multiple comparisons analysis on the slope of the biodiversity-ecosystem functioning relationship by temperature fluctuation treatment and time.

Step	Model	n par	χ^2	df	p-value	R^2m	R^2c	AIC	ΔAIC	AIC weight
0	Intercept+(1|id)	3				0.00	0.52	8,292	213	0.000
1	T+(1|id)	5	77.7	2	1.3e-17	0.05	0.52	8,218	140	0.000
2	T+D+(1|id)	6	6.8	1	9.1e-03	0.05	0.52	8,213	135	0.000
3	T+D+ln(R)+(1|id)	7	88.3	1	5.5e-21	0.10	0.52	8,127	48	0.000
4	T+D+T*ln(R)+(1|id)	9	2.1	2	3.4e-01	0.10	0.52	8,129	50	0.000
5	T+D+T*ln(R)+D*ln(R)+(1|id)	10	0.5	1	4.7e-01	0.10	0.52	8,130	52	0.000
6	T+D+T*ln(R)+D*ln(R)+D*T+(1|id)	12	42.8	2	5.2e-10	0.10	0.54	8,092	13	0.001
7	**T+D+T*ln(R)+D*ln(R)+D*T+D*T*ln(R)+(1|id)**	**14**	**17.0**	**2**	**2.0e-04**	**0.11**	**0.54**	**8,078**	**0**	**0.999**

to thermal stress should increase with species richness.

A second mechanism that could drive the BEF slopes is a change in the strength of interspecific competition. Indeed, our theoretical model showed that the BEF slope can change with the strength of interspecific competition, with a gradual decrease of the slope with increasing competition coefficient α (Fig. 4a, Appendix 1). We thus used the experimental data at day 15 to test whether potential changes in competitive interactions might have driven the observed results. If the change in BEF slope with temperature fluctuation treatment was linked to competitive interactions, we expected to observe a difference in interaction strength between species depending on the temperature fluctuation treatment, and we expected that the average interaction strength measured in each temperature treatment would interact with biodiversity to drive ecosystem function. This was not the case in our experiment, as interaction strength did not differ between treatments (Anova $F_{1,159} = 2.22$, $p = 0.11$, Fig. S6) and there was no interaction between richness and mean interaction strength on ecosystem functioning (value for the interaction $F_{1,1256} = 0.82$, $p = 0.36$). It is interesting to note that our model did not need a change in interaction strength to explain our experimental results, as using the average competition coefficient α estimated in the experiment (Fig. S6) was enough for the model predictions to fall within the 95% confidence intervals of the experimental slopes (Fig. 4b, Fig. S7).

Finally, a third mechanism is the insurance effect, whereby species fluctuate asynchronously depending on the environmental conditions. Our experimental data did not allow to test this mechanism, as getting full time-series data on all communities was too challenging logistically, however our model allowed an exploration of this mechanism. Following this hypothesis, we should expect that species' abundance should fluctuate asynchronously with temperature fluctuation depending on species' thermal tolerance, and that such asynchronous fluctuations should lead to higher ecosystem functioning with higher diversity. However, our model did not show such effect, as the few most abundant species, driving ecosystem functioning, were all fluctuating in synchrony

with temperature fluctuations, preventing the insurance effect from operating (Fig. S12).

Discussion

Temperature variability affected the relationship between biodiversity and ecosystem functioning. We demonstrated that larger temperature fluctuations led to a steeper relationship between phytoplankton biodiversity and production over time. We used a simple theoretical competition model to help understanding the mechanisms driving differences in the biodiversity-ecosystem functioning relationship across environments with distinct thermal fluctuations. It is to note that our theoretical model does not allow us to accept or reject a specific mechanism, but to explore the relative contribution of different mechanisms to the experimental results. We found that a likely mechanism might be the spread of species' thermal tolerances (i.e., interspecific variation in thermal tolerances). The reason is twofold. First, the contribution of species to community functioning in our experiment was linked to their thermal traits. Second, biodiversity-ecosystem functioning relationships in both the experiment and the model were linked to the spread of species' thermal tolerances. However, we did not find any indication of a change in competitive interactions with temperature fluctuation in our experiment, and no effect of experimentally measured competition strength on the BEF slope, suggesting that this mechanism was not at play here, although our study did not allow us to test this mechanism more rigourously. Similarly, we did not find support for asynchronous fluctuations among species as a mechanism explaining our results.

Ecosystem functioning increased with species richness through a linear relationship on log-log scale. The intercept of this relationship indicates ecosystem production at low levels (one species) of richness. The steepness of the slope elucidates the importance of biodiversity for ecosystem functioning. We found that temperature fluctuations decreased ecosystem production in species-poor communities. This was due to non-linear averaging of thermal tolerances. Indeed, because phytoplankton species were in the concave part of their thermal tolerance curve, the time-averaged tolerance in fluctuating conditions was lower than the tolerance at a constant average temperature (61, 62). Further, the biodiversity-ecosystem functioning slope was steeper over longer timescales in the moderate and severe thermal fluctuation treatment. This indicates that for the same decrease in species richness, ecosystem production decreased more in severely fluctuating environments. Interestingly, the magnitude of the change in slope was quite important, with a 91% increase in slope between the constant and severe fluctuations treatments, higher than the 53 % increase in slope with a 6°C temperature increase in (48), and the 44 % increase in slope with a 5°C temperature increase in (22). Future meta-analysis should aim at understanding which environmental drivers linked to climate change (e.g. changes in temperature mean, variance, or frequency of extreme climatic events) have the stronger impact on the BEF slope. In addition, ecosystem functioning for the communities of maximum diversity did not change across temperature treatments over time, suggesting that a greater diversity (12 species relative to 1) was able to compensate for the negative impact of larger environmental fluctuations.

We further found that the slope of the biodiversity-ecosystem function relationship changed through time. This agrees with studies on plant communities that found that the impact of biodiversity on ecosystem functioning increases through time (55, 56, 58, 63–67). This temporal increase of the BEF slope could arise from an increase in the productivity of the high richness communities over time (55), a decrease in the productivity of the low richness communities (57), or different rates of increase or decrease over time in the high and low richness communities (58). In our experiment, the temporal increase in slope depended on the temperature fluctuation treatment and on the measure for ecosystem production considered: while it was present for the moderate and severe fluctuating treatment when using abundance as a measure, it was present only for the severe fluctuation treatment when using biomass and for both constant and severe fluctuating treatments using chlorophyll *a* as a measure. Further, the reason for the increase in slope also depended on the metric used: for abundance, it was due to a decrease in the production of the one-species communities, with no temporal effect in the twelve-species communities. For

biomass, there was a decrease in the production in one-species communities in the stable and severely fluctuating treatment, but in twelve-species communities, ecosystem function actually increased with time in the two fluctuating treatments. Finally, for chlorophyll *a* it was due to an increase in production over time for all treatments at both richness levels, but a steeper increase in the production of the twelve-species communities. The dependency of the temporal effect on the ecosystem metric considered is in line with other studies, showing that changes at either low or high richness communities can drive the slope depending on the ecosystem function considered (58). Our study focused on abundance/biomass production as a measure of ecosystem functioning, however further studies should aim at understanding whether other ecosystem functions, such as such as C fixation, O_2 production, or nutrient recycling, would also lead to steeper BEF slopes with increased fluctuations. More interestingly, the effect of time varied with temperature fluctuation treatments, with a lower abundance over time in the low-richness communities in the severe fluctuating treatment but no effect in the constant temperature treatment. It is to note that our experiment was of short temporal duration (15 days). However given the fast reproductive rate of phytoplankton (around 0.9 generation per day on average), it encompassed a larger number of generations than most of the experiments on terrestrial plants reviewed in (55), where the median experiment length was 730 days, or ~2 generations of perennial plant species. Overall, our results show that as in grassland communities (66), increases in slopes seem to be due to both increases in production at high richness and decreases in production at low richness, and further show that the reason behind the strengthening of the biodiversity-ecosystem relationship over time might depend on the environmental context, and specifically on the temperature fluctuation level.

We investigated theoretically the variation in the biodiversity-ecosystem functioning slope with temperature fluctuations. Using a simple Lotka-Volterra competition model at steady state, we found that the strength of the biodiversity-ecosystem functioning slope depended on two fundamental parameters: the spread of species' thermal tolerances in the species pool, and competition strength. Parameterising the model with thermal tolerance curves for growth measured for these species by Barton and Yvon-Durocher (60), and with a competition coefficient directly estimated from the experiment, we obtained BEF slopes similar to those in our experiment. The steeper slopes characteristic of the severe fluctuation treatment were linked to the variability in the thermal tolerance of the species composing the communities. Indeed, species that had higher thermal tolerances in fluctuating conditions were also the ones that contributed the most to ecosystem functioning. Further, the spread in thermal tolerances in the species pool interacted with biodiversity to drive ecosystem functioning in our experiment. Thus, as suggested by our theoretical model, species pools with a larger spread of thermal traits were better able to cope with the increasing temperature fluctuations, leading to greater biodiversity-ecosystem functioning slopes.

Although our model shows that competition strength can potentially be a major factor in determining the strength of the biodiversity-ecosystem functioning relationship, with weaker competition leading to steeper BEF slopes, our experimental results suggest that this mechanism was not an important driver here. Indeed, we found no effect of temperature fluctuations on competition strength in the experiment, and no interaction between competition strength and biodiversity on ecosystem functioning. Further, using the average value of competition strength across treatments we accurately predicted the experimental BEF slope, suggesting that a change in competitive interactions was not needed to explain our results. Importantly, our model assumes that interaction structure between species is symmetric, while this might not be the case in the experiment. Indeed, some species might be better competitors regardless of their thermal tolerance, and thermal tolerance could further affect competitive abilities (68). Our experimental communities showed some variation in relative interaction intensity including some facilitative interactions (Fig. S6), which might contribute to some unexplained variation in the BEF slope. Thus we cannot fully reject the hypothesis that variation in species interaction strength might affect the BEF slope, although the spread in

thermal tolerances seems to be the strongest driver.

Interestingly, while the temporal insurance hypothesis posits that the slope of the biodiversity-ecosystem functioning relationship should be steeper in temporally variable environments due to different species dominating the community dynamics through time (5), our theoretical model suggests that such a mechanism might not be an important driver here, although we did not have experimental results to support this hypothesis. Indeed, the most abundant species fluctuated in synchrony with each other in response to the environmental conditions, with no sign of asynchrony that could lead to greater ecosystem function overall. In our model, the species that had the larger average growth rate over the two temperature conditions dominated the community all the time, and such time-averaged growth rate was linked to greater contribution to community functioning in the experimental results.

The purpose of our model was to explore the mechanisms operating in the experiment. To do so, we made a number of simplifications. In particular, the model assumes equilibrium in which nutrient renewal is constant, while nutrients in our experiment are only added at the beginning. Relaxing this assumption, we found that the model results depend on the rate of nutrient depletion (Appendix 1, Fig. S13). We show that communities reach a quasi-equilibrium that coincides with the Lotka-Volterra equilibrium, and remain in this state for a time that depends on the rate of nutrient uptake, until a sharp decrease in abundances when nutrients are completely exhausted in the environment. In our experiment, it is likely that species were at stationary growth phase and thus carrying capacity by day 15 (Fig. S14), and thus the simple Lotka-Volterra equilibrium might be a good approximation of the reality.

Our experimental results contrast with those of Parain *et al.* (49) on protozoan-bacteria consumer-resource communities. The authors found a decrease in the BEF slope value with increased mean and variation of temperature. Using a similar competition model to the one developed here, they found that the mechanism behind their results was a temperature-induced increase in consumer attack rates, which translated into higher effective competitive interactions among consumers. Baert *et al.* (51) showed theoretically and empirically that the slope of the biodiversity-ecosystem functioning had a hump-shaped relationship with environmental stress. In their study, the BEF slope increased from low to medium values of environmental stress due to the increased probability that more diverse communities contain a stress-tolerant species. However, when stress levels were high, the BEF relationship collapsed into a horizontal line as stress was sufficiently high to inhibit the growth of all species. This effect was comfounded by changes in species interactions that are more idiosyncratic and might depend on species identities, making predictions more difficult. In our system, thermal fluctuations can be considered an environmental stress, as evidenced by the strongly decreased effective growth rate in almost all species in the severe fluctuation treatment (Fig. S5). However, our extreme (i.e., 19-31°C) fluctuation treatment was not sufficiently high to inhibit the growth of all species, explaining the steeper slope with increasing temperature fluctuation. Overall, temperature fluctuations can lead to drastically different responses of the biodiversity-ecosystem functioning relationship depending on whether it leads to a change in species interactions or is driven by differences in thermal tolerances. A better understanding of the conditions in which increased temperature variability leads to one, the other, or a mix of both is needed in order to predict ecosystem responses in the face of climate change and biodiversity loss. Simple competitive models such as ours, Parain *et al.* (49), or Baert *et al.* (51) can help understanding whether and when species traits affect biodiversity-ecosystem functioning relationships.

Conclusion

The combination of rapid climate change and human-driven biodiversity loss makes understanding how changing climatic conditions and biodiversity levels will affect ecosystem functioning an imperative. Our proof-of-concept study showed both experimentally and theoretically that due to variation in phytoplankton species thermal tolerances, thermal fluctuations affected the slope of the relationship between biodiversity and ecosystem functioning. When climatic

conditions fluctuate strongly, the slope of the relationship is steeper, suggesting that biodiversity loss has a stronger negative effect on ecosystem functioning than when the environment is more stable. This is particularly true over longer timescales, as the slope of the relationship becomes steeper over time in the severe fluctuation treatment. Changes in biodiversity-ecosystem functioning slope were primarily linked to differences and variability in thermal tolerances. Although, theoretically, modifications in competitive interactions can also play a role, we found no support for this mechanism and neither for the effect of asynchronous populations fluctuations. Because climate change entails both changes in the mean and variance in temperature and because increased temperatures have also been found to increase the slope of the biodiversity-ecosystem functioning relationship, we should now understand the potential for interactive effects between mean and temperature fluctuations. Further studies should also aim at scaling-up our results to more complex communities and ecosystems (69), taking into account trophic diversity as well as more realistic mesocosm and natural settings increasing the spatial and temporal scale.

Materials and Methods

Species and culture conditions

We used 12 species of marine phytoplankton for the experiment, *Amphidinium carterae, Bigelowiella natans, Dunaliella tertiolecta, Emiliania huxleyi, Gymnochlora stellata, Ostreococcus tauri, Porphyridium aerugineum, Porphyridium purpureum, Phaeodactylum tricornutum, Rhodella maculata, Synechocystis sp* and *Thoracosphaera heimii*. These species encompass most of the biogeochemically and ecologically important groups (Chlorophytes, Coccolithophores, Cyanobacteria, Diatoms, Dinoflagellates, Rhodophytes and Prasinophytes; Table S12). Strains of each species were sourced from an experiment run at Exeter University (United Kingdom) by Barton and Yvon-Durocher (60), in which the authors studied thermal tolerance curves for growth of culture collection strains of 18 marine phytoplankton species including these 12 species. Stocks of each of the strains were transferred from Exeter University to the Station d'Ecologie Théorique et Expérimentale (Moulis, France). Species were cultured on Keller's K + Si medium in a Panasonic MLR-352 incubator at 20°C on a 12:12 light-dark cycle with a light intensity of 50 $\mu mol \cdot m^{-2} \cdot s^{-1}$, and kept under nutrient replete, exponential growth conditions by transferring 1 ml of each culture into new medium every week for ~3 months before the experiment.

Biodiversity-Ecosystem functioning experiment

We created artificial communities using the random partition design described by Bell *et al.* (59) to study how the relationship between biodiversity and ecosystem functioning varied with temperature fluctuations. We randomly combined species into communities with different species richness levels from 1, 2, 3, 4, 6, and 12 species. At each species richness level, we constructed the community assemblages by sampling all of the 12 species without replacement (Fig. 1), allowing each species to be represented an equal number of times (22). We repeated the sampling 5 times to form 5 independent partitions of the species pool, so that the number of assemblages for each richness level (R) was 5 x 12/R. We then replicated each assemblage 3 times. We subjected all replicated communities to three temperature fluctuation treatments, constant 25°C, fluctuating between 22 and 28°C and fluctuating between 19 and 31°C, which led us to get a total of 3 x 3 x 5 x (12 + 6 + 4 + 3+ 2 + 1) = 1260 communities for the whole experiment.

We used fifty-four 24 well plates (18 plates per temperature) filled with 2 mL of K+Si medium to create the experimental communities. We inoculated each well with 1200 $cells.mL^{-1}$ of each community (i.e. 100 $cells.mL^{-1}$ per species for twelve-species communities, 200 $cells.mL^{-1}$ per species for six-species communities, 300 $cells.mL^{-1}$ per species for four-species communities, 400 $cells.mL^{-1}$ per species for three-species communities, 600 $cells.mL^{-1}$ per species for two-species communities, and 1200 $cells.mL^{-1}$ per species for monocultures). We randomised the position of the communities within the plates.

To minimise evaporation and contamination within the wells while allowing gas exchange, we covered plates with AeraSeal breathable membrane. We then grew the communities in three Panasonic incubators on a 12:12

light:dark cycle at either constant 25°C temperature, fluctuation every other day between 22 and 28°C, or fluctuation every other day between 19 and 31°C. To refill water loss due to evaporation, we added 0.4 ml of distilled water every 2-3 days to each well. After 5 and 15 days of experiment, we sampled 100 µL from each community onto a 96 well plate. We chose these two time points based on the data collected by Barton and Yvon-Durocher (60), whose growth curves collected at temperatures close to our experimental temperatures showed that species were likely in their exponential phase of growth at day 5, while they should reach stationary phase of growth by day 15 (Fig S14). Samples were preserved with 10 µL of 1% sorbitol solution as a cryoprotectant, incubated one hour in the dark, and then frozen at -80°C until further analysis. Plates were defrosted and we determined total cell density in each sample by flow cytometry (BD FACSCanto II HTS). Plates were run on the flow cytometer on 0.5 $\mu L \cdot sec^{-1}$ flow rate, with three times 50 µL mixing and a cleaning of 400 µL between each sample to avoid contamination of measurements between samples.

Data analyses

We extracted flow cytometry standard (FSC) files from the flow cytometer into R v3.5.3 (70) using the Bioconductor package *FlowCore* to get cell counts and the associated cytometric properties (forward scatter (FSC, a proxy of size), side scatter (SSC), and far red fluorescence (PerCP.Cy5, a proxy of chlorophyll *a* content)). We first filtered the data to remove noise by removing every data point where $\log_{10}(\text{PerCP.Cy5})<1.5$, $\log_{10}(\text{FSC})<3.3$ and $\log_{10}(\text{SSC})<1.5$, which were below minimum values observed for live cells of these species. We then used the calibration curves described in Appendix 2 to estimate cell chlorophyll *a* content in $pg.cell^{-1}$ from PerCP.Cy5 values and cell biomass in $pgC.cell^{-1}$ from FSC values.

We calculated community abundance as the total number of cells per mL and total biomass and chlorophyll *a* content as the sum of biomass or chlorophyll *a* across all cells scaled to numbers per mL. Because the theoretical model we present focuses on growth rate and abundance, we present the cell abundance data in the main text, and use this metric as a measure of ecosystem functioning. However, similar results are found with the total chlorophyll *a* content and total biomass, presented in supplementary materials.

We used linear mixed models with lme4 package to understand how the relationship between biodiversity and ecosystem functioning (BEF) varied with time and temperature fluctuation treatment. We first fitted a linear mixed model of log-abundance against the temperature fluctuation treatments as a factor as well as a random effect of sample identity to account for non-independence between time points, and we added sequentially day of sampling (as a factor, day 5 or day 15), log-transformed species richness, and the two-way and three-way interactions between the three factors. We compared models of increasing complexity with AIC. The best model included the triple interaction between time, temperature fluctuation treatment and log species richness. We used post-hoc contrasts to assess whether the BEF slope differed between each pairwise combination of temperature fluctuation treatment levels for a given date with *emtrends* function from *emmeans* package adjusting p-values with Tukey method. We also tested whether the BEF slope differed between the two dates for each temperature fluctuation treatment level with the same methods.

In a second step, we aimed to understand whether ecosystem function depended on species thermal tolerances, measured for growth by Barton and Yvon-Durocher (60)'s experiment. Tolerance was calculated as either the growth rate at 25°C for the constant treatment or the average of the growth rates at 22 and 28°C (resp. 19 and 31°C, hereafter named effective growth rate) for the fluctuating treatments (Fig. S5). Using the average of the two temperatures is reasonable because the change in the temperature in the incubators is very fast (from 19°C to 31°C and conversely in <20 minutes). We first measured the spread in thermal tolerances in the species pool for each temperature fluctuation level as the difference between the maximum and the minimum effective growth rate scaled by maximum effective growth rate. We then assessed whether such spread affected BEF relationship by modelling ecosystem functioning at day 15 as a function of the interaction between spread in thermal tolerance and log richness in a linear

model. To test whether results were congruent with different measures of spread, we redid the analysis using the coefficient of variation of species thermal tolerance. Second, we assessed whether each species' contribution to ecosystem functioning was linked to their thermal tolerance. We used the residuals from the best supported model of the first step (Table 1) to fit a linear mixed model of community composition, with 12 variables representing each species' presence-absence status, and their interaction with temperature as a factor, as well as sample identity as a random effect. This method provides species coefficients that allow understanding the effect of each species on ecosystem functioning relative to an average species (59). Species with positive coefficient contribute to ecosystem functioning above the average species, while negative coefficients show a below-average contribution. We used a linear model to link these species coefficients to each species' thermal tolerance.

We also aimed at evaluating interspecific competition strength in the experiment. To do so, we used a random forest classification algorithm to discriminate cells from each species in each two-species community and calculate relative abundance at day 15 and thus to calculate abundance of each species within the two-species communities (Appendix 3). We then calculated pairwise species interactions by the relative interaction intensity index (RII, (71)) from the ratio of the difference and sum of abundance of the species in monoculture B_o and the abundance of the species in polyculture B_w, $RII = \frac{B_w - B_o}{B_w + B_o}$. Note that because total initial abundance was kept constant across diversity levels (as usual in biodiversity-ecosystem functioning experiments), we can only use RII at day 15. We first tested whether RII varied with temperature fluctuation treatment with an ANOVA. We then tested whether RII affected BEF relationship by modelling ecosystem functioning as a function of the interaction between log richness and average RII in each temperature fluctuation treatment.

Theoretical model

Model definition

We constructed a model to generate predictions and test mechanisms for the biodiversity-ecosystem functioning slope at different levels of thermal fluctuation. The model is based on the competitive Lotka-Volterra equations, which describe the dynamics of species abundance N_i, where species index i runs over S species

$$\frac{dN_i}{dt} = r_i N_i - \sum_j a_{ij} N_i N_j$$

The model parameters are r_i, the intrinsic growth rate of species i, and a_{ij} is the competition strength of species j on species i. To keep the model parameterisable, we assumed symmetric competition, i.e., all intraspecific competition strengths are equal, $a_{ii} = a_0$ for all i, and all interspecific competition strengths are equal, $a_{ij} = a_1$ for all i and j with $i \neq j$. Environmental conditions affects intrinsic growth rates r_i, and potentially also interaction strengths a_0 and a_1. Despite its simplicity this model has been shown to provide insights in the effects of a changing environment on the BEF relationship (49, 51).

Model analysis

We investigated how the slope of the relationship between log species richness and log community abundance depends on the model parameters (see Appendix 1). Our model focuses on community abundance at steady state, which we considered to correspond to the day 15 conditions in the experiments, as single-species growth curves show that species are at stationary growth phase and thus carrying capacity by day 15 (Fig. S14). Further, it is to note that although in principle steady state of communities and ecosystems can differ strongly from steady state of the one-species population dynamics, in our model these different steady states are reached at similar times. We found that at steady state, the BEF slope is determined by only two model features: (i) the spread of intrinsic growth rates between species, and (ii) the ratio of inter- to intraspecific competition strength, $\alpha = a_1 / a_0$. Moreover, this result remains approximately valid for the treatments with thermal fluctuations. It suffices to replace the model parameters r_i, a_0 and a_1 by their average over the two temperatures of the fluctuation treatment. Note that we focus our theoretical analysis on production at steady state as it does not depend on initial biomass conditions

(Appendix 1) and is hence more easy to verify than the prediction for the transient regime, which is affected by both the model parameters and the initial conditions.

The key parameters of our model are instances of the two broad categories of coexistence mechanisms (52, 53, 72). In analogy with coexistence theory we denote the spread of intrinsic growth rates, either at a fixed temperature for the constant treatment or averaged over two temperatures for the fluctuation treatments, "tolerance differences". The ratio of inter- to intraspecific competition strength α, sometimes called the competition coefficient, determines "niche differences", which are small for $\alpha \approx 1$ and large for $\alpha \approx 0$.

The model predicted the following dependencies of the BEF slope on the two key model parameters (see Fig. S9). If all species have approximately the same growth rate (weak tolerance differences), then the BEF slope decreases gradually from one at $\alpha = 0$ (non-overlapping niches, no interspecific competition) to zero at $\alpha = 1$ (no niche differences, interspecific competition equal to intraspecific competition). In case of strong tolerance differences, the BEF slope decreases more slowly from one at $\alpha = 0$ towards a lower value at $\alpha = 1$.

Model parameterisation

To obtain a prediction for the BEF slope that can be compared to the experimental results, we estimated first the two key model parameters. We determined the intrinsic growth rates using the thermal tolerance curves measured by (60). For the constant treatment (25 °C) we set the intrinsic growth rates r_i equal to the tolerance measured at this temperature. For the variable treatments (22-28 °C and 19-31 °C), we took the average of the tolerances measured at the two temperatures of the fluctuation regime (Fig. S5). Note that under the model assumptions only relative values of species tolerance matter for the BEF slope (see Appendix 1).

We estimated the ratio of inter- to intra-specific competition using relative interaction intensities (RIIs, (71), Fig. S6). We computed the steady-state solution of the model for the same two-species communities that were used to determine the empirical distribution of RIIs. We repeated this computation for a range of values of the competition coefficient α. These results allowed us to establish a relationship between α and the average RII, dependent on the empirically estimated intrinsic growth rates. By evaluating this relationship at the average of the empirical RII distribution, we obtained our estimate of the competition coefficient α. We then plugged in the estimates for the intrinsic growth rates and the competition coefficient α in the theoretical model. We used the same random partitioning design as in the experiment, to obtain 88 community compositions separated into 6 richness levels (R = 1, 2, 3, 4, 6 and 12 species). By regressing steady-state community abundance against initial species richness on a log-log scale, we obtained our prediction for the BEF slope. Importantly, the data used to generate the theoretical prediction were largely independent from the data used to construct the empirical BEF relationship. The effective growth rates were from (60), and the competition coefficient was estimated from the individual species abundances in the two-species polycultures, while only the total community abundance matters for the BEF relationship.

Acknowledgements

This research is supported by the French ANR through LabEx TULIP (ANR-10-LABX-41) and by the FRAGCLIM Consolidator Grant, funded by the European Research Council under the European Union's Horizon 2020 research and innovation programme (Grant Agreement Number 726176). We thank Gabriel Yvon-Durocher for providing the algae for the experiment and Alexios Synodinos for comments on the manuscript.

Author contributions: EB conceived the study. EB and JMM designed the experiment. SB provided the phytoplankton strains and characterised their thermal tolerance. EB performed the biodiversity experiment with the help of SAC, AG, MH. EB analysed the data. BH conceived the theory. EB, BH and JMM interpreted the data and the data-theory convergence. EB wrote the manuscript. BH and JMM contributed to different revisions, with SB, SAC, AG, and MH contribution to final revisions. JMM financially managed the project, and obtained the funding. The authors declare no competing interests.

Data accessibility statement: Data and code are available on Zenodo : https:doi.org/10.5281/zenodo.5078310

References

1. IPCC, Climate change 2013: the physical science basis : Working Group I contribution to the fifth assessment report of the Intergovernmental Panel on Climate Change, T. F. Stocker, et al., Eds. (Cambridge University Press, 2013).

2. S. Díaz, et al., "Summary for policymakers of the global assessment report on biodiversity and ecosystem services – unedited advance version" in IPBES Global Assesment Report on Biodiversity and Ecosystem Services, (2019), p. 39.

3. D. F. Doak, et al., The Statistical Inevitability of Stability-Diversity Relationships in Community Ecology. The American Naturalist **151**, 264–276 (1998).

4. D. Tilman, The Ecological Consequences of Changes in Biodiversity: A Search for General Principles. Ecology **80**, 1455–1474 (1999).

5. S. Yachi, M. Loreau, Biodiversity and ecosystem productivity in a fluctuating environment: The insurance hypothesis. PNAS **96**, 1463–1468 (1999).

6. D. U. Hooper, et al., Effects of biodiversity on ecosystem functioning: a consensus of current knowledge. Ecological Monographs **75**, 3–35 (2005).

7. B. J. Cardinale, et al., Effects of biodiversity on the functioning of trophic groups and ecosystems. Nature **443**, 989–992 (2006).

8. D. Tilman, F. Isbell, J. M. Cowles, Biodiversity and Ecosystem Functioning. Annu. Rev. Ecol. Evol. Syst. **45**, 471–493 (2014).

9. J. M. Montoya, D. Raffaelli, Climate change, biotic interactions and ecosystem services. Philosophical Transactions of the Royal Society of London B: Biological Sciences **365**, 2013–2018 (2010).

10. G.-R. Walther, Community and ecosystem responses to recent climate change. Phil. Trans. R. Soc. B **365**, 2019–2024 (2010).

11. D. U. Hooper, et al., A global synthesis reveals biodiversity loss as a major driver of ecosystem change. Nature **486**, 105–108 (2012).

12. S. Naeem, J. E. Duffy, E. Zavaleta, The Functions of Biological Diversity in an Age of Extinction. Science **336**, 1401–1406 (2012).

13. F. Isbell, et al., Linking the influence and dependence of people on biodiversity across scales. Nature **546**, 65–72 (2017).

14. D. R. Easterling, et al., Climate Extremes: Observations, Modeling, and Impacts. Science **289**, 2068–2074 (2000).

15. L. W. Traill, M. L. M. Lim, N. S. Sodhi, C. J. A. Bradshaw, Mechanisms driving change: altered species interactions and ecosystem function through global warming. Journal of Animal Ecology **79**, 937–947 (2010).

16. T. Burgmer, H. Hillebrand, Temperature mean and variance alter phytoplankton biomass and biodiversity in a long-term microcosm experiment. Oikos **120**, 922–933 (2011).

17. N. B. Grimm, et al., The impacts of climate change on ecosystem structure and function. Frontiers in Ecology and the Environment **11**, 474–482 (2013).

18. B. Helmuth, et al., Beyond long-term averages: making biological sense of a rapidly changing world. Climate Change Responses **1**, 6 (2014).

19. D. A. Vasseur, et al., Increased temperature variation poses a greater risk to species than climate warming. Proc. R. Soc. B **281**, 20132612 (2014).

20. M. P. Thakur, et al., Climate warming promotes species diversity, but with greater taxonomic redundancy, in complex environments. Science Advances **3**, e1700866 (2017).

21. F. C. García, E. Bestion, R. Warfield, G. Yvon-Durocher, Changes in temperature alter the relationship between biodiversity and ecosystem functioning. PNAS **115**, 10989–10994 (2018).

22. E. Bestion, S. Barton, F. C. García, R. Warfield, G. Yvon-Durocher, Abrupt declines in marine phytoplankton production driven by warming and biodiversity loss in a microcosm experiment. Ecology Letters **23**, 457–466 (2020).

23. D. Zhong, L. Listmann, M.-E. Santelia, C.-E. Schaum, Functional redundancy in natural pico-phytoplankton communities depends on temperature and biogeography. Biology Letters **16**, 20200330 (2020).

24. C. D. Thomas, et al., Extinction risk from climate change. Nature **427**, 145–148 (2004).

25. M. D. Walker, et al., Plant community responses to experimental warming across the tundra biome. PNAS **103**, 1342–1346 (2006).

26. S. C. Elmendorf, et al., Global assessment of experimental climate warming on tundra vegetation: heterogeneity over space and time. Ecology Letters **15**, 164–175 (2012).

27. M. C. Urban, Accelerating extinction risk from climate change. Science **348**, 571–573 (2015).

28. J. J. Wiens, Climate-Related Local Extinctions Are Already Widespread among Plant and Animal Species. PLOS Biology **14**, e2001104 (2016).

29. E. Bestion, et al., Climate warming reduces gut microbiota diversity in a vertebrate ectotherm. Nature Ecology & Evolution **1**, 0161 (2017).

30. L. H. Antão, et al., Temperature-related biodiversity change across temperate marine and terrestrial systems. Nature Ecology & Evolution, 1–7 (2020).

31. J. García Molinos, et al., Climate velocity and the future global redistribution of marine biodiversity. Nature Climate Change **6**, 83–88 (2016).

32. A. Gonzalez, et al., Estimating local biodiversity change: a critique of papers claiming no net loss of local diversity. Ecology **97**, 1949–1960 (2016).

33. D. S. Gruner, et al., Effects of experimental warming on biodiversity depend on ecosystem type and local species composition. Oikos **126**, 8–17 (2017).

34. B. J. Cardinale, A. Gonzalez, G. R. H. Allington, M. Loreau, Is local biodiversity declining or not? A summary of the debate over analysis of species richness time trends. Biological Conservation **219**, 175–183 (2018).

35. A. J. Suggitt, D. G. Lister, C. D. Thomas, Widespread Effects of Climate Change on Local Plant Diversity. Current Biology **29**, 2905-2911.e2 (2019).

36. M. Vellend, et al., Global meta-analysis reveals no net change in local-scale plant biodiversity over time. Proceedings of the National Academy of Sciences **110**, 19456–19459 (2013).

37. M. Dornelas, et al., Assemblage Time Series Reveal Biodiversity Change but Not Systematic Loss. Science **344**, 296–299 (2014).

38. J. B. Shurin, et al., Environmental stability and lake zooplankton diversity – contrasting effects of chemical and thermal variability. Ecology Letters **13**, 453–463 (2010).

39. S. Schabhüttl, et al., Temperature and species richness effects in phytoplankton communities. Oecologia **171**, 527–536 (2013).

40. S. Rasconi, K. Winter, M. J. Kainz, Temperature increase and fluctuation induce phytoplankton biodiversity loss – Evidence from a multi-seasonal mesocosm experiment. Ecology and Evolution **7**, 2936–2946 (2017).

41. Y. Zhang, et al., Climate variability decreases species richness and community stability in a temperate grassland. Oecologia **188**, 183–192 (2018).

42. M. Gerhard, A. M. Koussoroplis, H. Hillebrand, M. Striebel, Phytoplankton community responses to temperature fluctuations under different nutrient concentrations and stoichiometry. Ecology **100**, e02834 (2019).

43. L. Rustad, et al., A meta-analysis of the response of soil respiration, net nitrogen mineralization, and aboveground plant growth to experimental ecosystem warming. Oecologia **126**, 543–562 (2001).

44. Z. Wu, P. Dijkstra, G. W. Koch, J. Peñuelas, B. A. Hungate, Responses of terrestrial ecosystems to temperature and precipitation change: a meta-analysis of experimental manipulation. Global Change Biology **17**, 927–942 (2011).

45. G. Yvon-Durocher, et al., Five Years of Experimental Warming Increases the Biodiversity and Productivity of Phytoplankton. PLoS Biol **13**, e1002324 (2015).

46. A. Zander, L.-F. Bersier, S. M. Gray, Effects of temperature variability on community structure in a natural microbial food web. Glob Change Biol, n/a-n/a (2016).

47. L. A. Domeignoz-Horta, et al., Microbial diversity drives carbon use efficiency in a model soil. Nature Communications **11**, 3684 (2020).

48. B. Steudel, et al., Biodiversity effects on ecosystem functioning change along environmental stress gradients. Ecol Lett **15**, 1397–1405 (2012).

49. E. C. Parain, R. P. Rohr, S. M. Gray, L.-F. Bersier, Increased Temperature Disrupts the Biodiversity–Ecosystem Functioning Relationship. The American Naturalist **193**, 227–239 (2019).

50. A. L. Gonçalves, M. A. S. Graça, C. Canhoto, Is diversity a buffer against environmental temperature fluctuations? – A decomposition experiment with aquatic fungi. Fungal Ecology **17**, 96–102 (2015).

51. J. M. Baert, N. Eisenhauer, C. R. Janssen, F. D. Laender, Biodiversity effects on ecosystem functioning respond unimodally to environmental stress. Ecology Letters **21**, 1191–1199 (2018).

52. I. T. Carroll, B. J. Cardinale, R. M. Nisbet, Niche and fitness differences relate the maintenance of diversity to ecosystem function. Ecology **92**, 1157–1165 (2011).

53. J. W. Spaak, F. De Laender, Intuitive and broadly applicable definitions of niche and fitness differences. Ecology Letters **23**, 1117–1128 (2020).

54. C. L. Lehman, D. Tilman, Biodiversity, Stability, and Productivity in Competitive Communities. The American Naturalist **156**, 534–552 (2000).

55. B. J. Cardinale, et al., Impacts of plant diversity on biomass production increase through time because of species complementarity. PNAS **104**, 18123–18128 (2007).

56. P. B. Reich, et al., Impacts of Biodiversity Loss Escalate Through Time as Redundancy Fades. Science **336**, 589–592 (2012).

57. E. Marquard, et al., Changes in the Abundance of Grassland Species in

Monocultures versus Mixtures and Their Relation to Biodiversity Effects. PLoS One **8** (2013).

58. S. T. Meyer, et al., Effects of biodiversity strengthen over time as ecosystem functioning declines at low and increases at high biodiversity. Ecosphere **7**, e01619 (2016).

59. T. Bell, et al., A Linear Model Method for Biodiversity–Ecosystem Functioning Experiments. The American Naturalist **174**, 836–849 (2009).

60. S. Barton, G. Yvon-Durocher, Quantifying the temperature dependence of growth rate in marine phytoplankton within and across species. Limnology and Oceanography **64**, 2081–2091 (2019).

61. J. R. Bernhardt, J. M. Sunday, P. L. Thompson, M. I. O'Connor, Nonlinear averaging of thermal experience predicts population growth rates in a thermally variable environment. Proceedings of the Royal Society B: Biological Sciences **285**, 20181076 (2018).

62. L. E. Dee, D. Okamtoto, A. Gårdmark, J. M. Montoya, S. J. Miller, Temperature variability alters the stability and thresholds for collapse of interacting species. bioRxiv, 2020.05.18.102053 (2020).

63. D. Tilman, et al., Diversity and Productivity in a Long-Term Grassland Experiment. Science **294**, 843–845 (2001).

64. J. van Ruijven, F. Berendse, Long-term persistence of a positive plant diversity–productivity relationship in the absence of legumes. Oikos **118**, 101–106 (2009).

65. J. M. Ravenek, et al., Long-term study of root biomass in a biodiversity experiment reveals shifts in diversity effects over time. Oikos **123**, 1528–1536 (2014).

66. N. R. Guerrero-Ramírez, et al., Diversity-dependent temporal divergence of ecosystem functioning in experimental ecosystems. Nature Ecology & Evolution **1**, 1639–1642 (2017).

67. W. W. Weisser, et al., Biodiversity effects on ecosystem functioning in a 15-year grassland experiment: Patterns, mechanisms, and open questions. Basic and Applied Ecology **23**, 1–73 (2017).

68. E. Bestion, B. García-Carreras, C.-E. Schaum, S. Pawar, G. Yvon-Durocher, Metabolic traits predict the effects of warming on phytoplankton competition. Ecology Letters **21**, 655–664 (2018).

69. A. Gonzalez, et al., Scaling-up biodiversity-ecosystem functioning research. Ecology Letters **23**, 757–776 (2020).

70. R Core Team, R: A Language and Environment for Statistical Computing (R Foundation for Statistical Computing, 2019).

71. C. Armas, R. Ordiales, F. I. Pugnaire, Measuring Plant Interactions: A New Comparative Index. Ecology **85**, 2682–2686 (2004).

72. P. Chesson, Mechanisms of Maintenance of Species Diversity. Annual Review of Ecology and Systematics **31**, 343–366 (2000).

Supplementary Material

Table of contents

Appendix 1: Model analysis

Here we present a detailed analysis of the Lotka-Volterra model (1) presented in the main text. Assuming symmetric competition, the model reads

$$\frac{dN_i}{dt} = r_i N_i - a_0 N_i^2 - \sum_{j \neq i} a_1 N_i N_j$$

$$= N_i (r_i - a_0 N_i - a_1 \textstyle\sum_{j \neq i} N_j) \qquad \text{(S1)}$$

The parameter r_i can be interpreted as the species' tolerance for the current environment. A highly tolerant species is assumed to have both a large intrinsic growth rate r_i (i.e. its growth rate in the absence of con- and heterospecific competitors) and a large carrying capacity r_i/a_0 (i.e., its equilibrium abundance in the absence of heterospecific competitors).

The model parameters r_i, a_0 and a_1 depend on temperature. We take the same temperature dependencies for the constant and fluctuation treatments. That is, we assume that in case of fluctuating temperature, growth and competition take the same values as if the instantaneous temperature persisted since a long time. This assumption holds if the temperature fluctuations are relatively slow compared to the thermal response of the individual organisms (i.e., the organisms' physiological response).

We are interested in the steady-state dynamics, in which species abundance fluctuate periodically, with the same period as the temperature. In general, the steady state can be studied by numerically solving the dynamical equations (S1). However, one steady-state property can be studied directly: the time average of the species abundances. Indeed, denoting the time average by an overline, we have

$$0 = \overline{\frac{d \ln N_i}{dt}} = \overline{\frac{1}{N_i} \frac{dN_i}{dt}}$$

$$= \overline{r_i} - \overline{a_0 N_i} - \overline{a_1 \sum_{j \neq i} N_j}$$

$$= \overline{r_i} - \overline{a_0}\,\overline{N_i} - cov(a_0, N_i) - \overline{a_1} \textstyle\sum_{j \neq i} \overline{N_j} - \sum_{j \neq i} cov(a_1, N_j)$$

$$\approx \overline{r_i} - \overline{a_0}\,\overline{N_i} - \overline{a_1} \textstyle\sum_{j \neq i} \overline{N_j} \qquad \text{(S2)}$$

where in the last line we neglected the covariance terms cov(a_0, N_i) and cov(a_1, N_j). These covariance terms are small if the temperature fluctuations are relatively fast compared the thermal response of the species abundances, i.e., if there is not sufficient time between temperature changes to lead to large abundance variation (i.e., the populations' ecological response). When this is the case, there is insufficient time between temperature changes to induce a large variation in abundance, and hence to create covariation between interaction strength and species abundance. If, on the contrary, the ecological response time is faster than the temperature fluctuation, approximation (S2) is less accurate. Both cases are illustrated in Fig. S15. Overall, ignoring these covariance terms introduces only a small error, especially when the time scale of the community dynamics is not much smaller than the fluctuation frequency, as is probably the case in our experiment.

Thus, we see that the steady-state conditions (S2) for the time-averaged species abundances N_i are closely related to equilibrium conditions for the species abundances N_i of the dynamical system (S1) without temperature fluctuations,

$$0 = r_i - a_0 N_i - a_1 \textstyle\sum_{j \neq i} N_j \qquad \text{(S3)}$$

These two sets of equations are equivalent if we replace the model parameters by their time-averaged values, i.e., r_i by $\overline{r_i}$, a_0 by $\overline{a_0}$ and a_1 by $\overline{a_1}$. Clearly, this equivalence is not strictly verified for our

experiment, given the numerous assumptions we made in its derivation. Still, it provides a useful approximation to study the effects of temperature fluctuations on the BEF relationship.

Next, we study the slope of the steady-state relationship between species diversity and community abundance. For simplicity, we formulate our analysis for the constant treatment. But by using the equivalence derived above, we can directly extend the results to the fluctuation treatments, provided we replace the model parameters by their time averages, and interpret the equilibrium as the time-averaged steady state.

We consider a species pool, where each species is characterized by an intrinsic growth rate r_i. From this pool we repeatedly sample subsets of species, put them into competition with competition strengths a_0 and a_1, and solve the steady-state species abundances N_i, see equation (S3). Regressing community abundance $\sum_i N_i$ against initial species richness R on a log-log plot, we obtain the slope of the BEF relationship.

The BEF slope predicted by the model satisfies some general properties. To derive them, we note that the predicted slope does not depend on the scale of species abundance used in the model. Indeed, if we multiply all species abundances by the same factor c, the BEF relationship of ln(total abundance) vs. ln(species richness) shifts vertically by the constant ln(c), but its slope remains unchanged. Introducing the factor c into equation (S3), we get

$$0 = r_i - c\, a_0 N_i - c\, a_1 \sum_{j \neq i} N_j$$

We set $c = r_{max}/a_0$, with r_{max} the largest species intrinsic growth rate. The equilibrium conditions can then be rewritten as

$$0 = \frac{r_i}{r_{max}} - N_i - \frac{a_1}{a_0} \sum_{j \neq i} N_j \qquad \text{(S4)}$$

Recalling that this rescaled equation predicts the same BEF slope as the original equation (S3), we see that (1) the predicted slope does not depend on the absolute species intrinsic growth rates, but on their relative spread, and (2) the predicted slope does not depend on the individual competition strengths a_0 and a_1, but on their ratio $\alpha = a_1 / a_0$.

We conclude that the BEF slope prediction is determined by only two model features: (1) the spread of intrinsic growth rates between species, called tolerance differences in the main text, and (2) the ratio of inter- to intraspecific competition strength, sometimes called competition coefficient. As explained above, these results immediately generalize to the case with temperature fluctuations, by replacing the model parameters by their time-averaged equivalents. The two key dependencies of the BEF slope are illustrated in Fig. S9.

Nutrient depletion and quasi-equilibrium

Our analysis of the Lotka-Volterra model is based on a steady-state assumption. In particular, we assumed that the equilibrium of the time-averaged model is comparable to the experimental data. Clearly, this assumption must break down when the nutrients become depleted (recall that we did not add nutrients during the experiment). Here we use a model with explicit nutrient dynamics to illustrate how the equilibrium of the Lotka-Volterra model can yield useful predictions even in the case of nutrient depletion.

We combine the Lotka-Volterra species interactions with simple nutrient dynamics. We assume that the decreasing pool of available nutrients can be described by a single nutrient density variable M. The coupled dynamics are

$$\frac{dN_i}{dt} = (g_i(M) - m_i)N_i - \sum_j b_{ij} N_i N_j$$

$$\frac{dM}{dt} = -\sum_i f_i(M)N_i \quad \text{(S5)}$$

Here $f_i(M)$ is the nutrient uptake rate (the functional response), $g_i(M)$ is the species growth rate (the numerical response), m_i is the species loss rate, and b_{ij} are competitive interaction strengths, excluding the part of competition mediated by nutrient M, because this part is modelled explicitly.

The functions $f_i(M)$ and $g_i(M)$ are typically saturating functions of nutrient density M. Using the Monod equation,

$$g_i(M) = \frac{c_i M}{k_i + M} \text{ and } f_i(M) = \frac{d_i M}{k_i + M}$$

Let us assume that at the start of the experiment, the functions f_i and g_i are at saturation, $g_i \approx c_i$ and $f_i \approx d_i$. Then the first part of the dynamics is described by

$$\frac{dN_i}{dt} = (c_i - m_i)N_i - \sum_j b_{ij}N_iN_j \quad \text{(S6)}$$

That is, during the initial phase the species abundances obey Lotka-Volterra dynamics (with $r_i = c_i - m_i$ and $a_{ij} = b_{ij}$). At a later time, different scenarios are possible (Fig. S13). The trajectories of the simple Lotka-Volterra dynamics and of the coupled model coincide until the nutrient density drops to a low level. If this drop occurs well after the Lotka-Volterra dynamics equilibrate, the species abundances in the coupled model reach a plateau, equal to the Lotka-Volterra equilibrium, and remain in this state for a relatively long time (Fig. S13a). This is a quasi-equilibrium, because the nutrient density continues to decrease, inducing eventually a decrease of the species abundances as well (Fig. S13b). If the nutrient drop occurs earlier, before the Lotka-Volterra equilibrate, the species abundances do not reach a quasi-equilibrium, but switch relatively quickly from an increasing to a decreasing slope (Fig. S13c). Growth curves from Barton and Yvon-Durocher (1) suggest that species are at stationary phase of growth by day 15, with no apparent decline in species abundances (Fig. S14). We conclude that the species abundances in a quasi-equilibrium can be approximated by a Lotka-Volterra equilibrium, justifying our modelling approach.

Appendix 2: Chlorophyll *a* and total biomass calibration

We separately grew each species, and at carrying capacity we calculated cell density and mean FSC and PerCP.Cy5 values on the flow cytometer as described in the main text. We then sampled 50 mL from each species and centrifuged them at 4°C at 3500 rpm for 30 minutes. We re-suspended the resultant pellets in 3 mL of ethanol (100%), and kept samples refrigerated in the dark for 24 hours to extract chlorophyll *a*. After that, we took two 200 µL technical replicates from each sample onto a 96 well plate to measure absorbance from 610 nm to 750 nm using a spectrophotometer (Tecan Spark 10M). We measured blanks across the same wavelength range to correct for the ethanol absorbance. We then obtained estimates of chlorophyll *a* in pg.cell^{-1} for the cultures using well established absorbance coefficients (2, 3) and dividing by cell abundance measured by flow cytometry. We used a linear model on a log-log scale to model the chlorophyll *a* values in pictograms per cell against mean PerCP.Cy5 values from the flow cytometer (estimates (± SE): intercept = -9.31 ± 1.75, slope: 0.805 ± 0.185, t = 4.35, p = 0.001, R^2 = 0.65). We finally used this calibration curve to estimate chlorophyll *a* content of the communities in the biodiversity-ecosystem function experiment from PerCP.Cy5 values from the flow cytometer. For biomass, we regressed measured cell diameter (d, µm^3) values from microscopy against FSC values from the flow cytometer using a linear model (estimates (± SE): intercept: -0.177 ± 0.487, slope = 2.2e-4 ± 2.1e-5, t = 10.3, p = 7e-10, R^2 = 0.83) and applied these calibration curves to the biodiversity-ecosystem function data. We then calculated the biovolume of each cell assuming that each particle was spherical ($biovolume = \frac{4}{3}\pi(\frac{d}{2})^3$) and converted into units of carbon (pg.cell^{-1}) using a conversion factor of ($biomass = 0.109\ biovolume^{0.991}$) derived from the literature (4–6). We finally summed biomasses across cells.

Appendix 3: Discrimination of cell identity in the two-species communities through random forest classification algorithm

We also aimed at evaluating interspecific competition strength in the experiment. To do so, we used a random forest classification algorithm to discriminate cells from each species in each two-species community and calculate relative abundance at 15 days. We used the values from the flow cytometry output to define species morphology and pigment composition and as inputs to the random forest analysis (7, 8). We used the monoculture dataset to create the random forest discrimination functions by separating it first into a training and a testing dataset. For each pre-existing two-species community composition in the polycultures (i.e. the 30 two-species pairs measured in the polycultures and not all of the 66 potential two-species pairs combinations possible with 12 species), we restricted the training and testing dataset to the two species present inside of the community. We used the variables returned by the flow cytometer (i.e. FSC, SSC, FITC, PE, PerCP.Cy5, PE.Cy7, APC, APC.H7, V450, V500) in the training dataset as input of the random forest algorithm to calculate discrimination functions between pairs of species. These discrimination functions were then used to predict species identity in the testing dataset. This allowed us to calculate for each simulated pair of species a percentage of accuracy in the prediction. Unfortunately, some species compositions led to very poor predictability (for instance, in the *Synechocystis sp* - *Thoracosphaera heimii* community, the abundance of *Thoracosphaera heimii* was poorly detected, with only 24.4 % of the cells correctly attributed to it). We therefore used a cut-off of community predictability, where the worst predicted species in the community would be predicted with at least 60 % of accuracy (8). This cut-off led us to exclude 3 out of the 30 pairs of species. The average prediction power for each species inside of the remaining 27 communities was 92 % ± 7 SD, which makes us confident in the assessed abundance of each species for these communities. We finally applied the discrimination algorithms to the two-species communities from the experiment (excluding the 3 communities for which the predictive power was below the threshold), and calculated each species abundance.

Appendix 4: References cited in the supplementary material

1. S. Barton, G. Yvon-Durocher, Quantifying the temperature dependence of growth rate in marine phytoplankton within and across species. *Limnology and Oceanography* **64**, 2081–2091 (2019).

2. R. J. Ritchie, Consistent Sets of Spectrophotometric Chlorophyll Equations for Acetone, Methanol and Ethanol Solvents. *Photosynth Res* **89**, 27–41 (2006).

3. M. Henriques, A. Silva, J. Rocha, Extraction and quantification of pigments from a marine microalga: a simple and reproducible method. *Commun. Curr. Res. Educ. Top. Trends Appl. Microbiol.*, 586–593 (2007).

4. D. J. S. Montagnes, J. A. Berges, P. J. Harrison, F. J. R. Taylor, Estimating carbon, nitrogen, protein, and chlorophyll a from volume in marine phytoplankton. *Limnology and Oceanography* **39**, 1044–1060 (1994).

5. D. Padfield, A. Buckling, R. Warfield, C. Lowe, G. Yvon-Durocher, Linking phytoplankton community metabolism to the individual size distribution. *Ecology Letters* **21**, 1152–1161 (2018).

6. C.-E. Schaum, *et al.*, Adaptation of phytoplankton to a decade of experimental warming linked to increased photosynthesis. *Nature Ecology & Evolution* **1**, 0094 (2017).

7. E. Bestion, B. García-Carreras, C.-E. Schaum, S. Pawar, G. Yvon-Durocher, Metabolic traits predict the effects of warming on phytoplankton competition. *Ecology Letters* **21**, 655–664 (2018).

8. E. Bestion, S. Barton, F. C. García, R. Warfield, G. Yvon-Durocher, Abrupt declines in marine phytoplankton production driven by warming and biodiversity loss in a microcosm experiment. *Ecology Letters* **23**, 457–466 (2020).

9. C. Armas, R. Ordiales, F. I. Pugnaire, Measuring Plant Interactions: A New Comparative Index. *Ecology* **85**, 2682–2686 (2004).

Appendix 5: Supplementary Figures and Tables

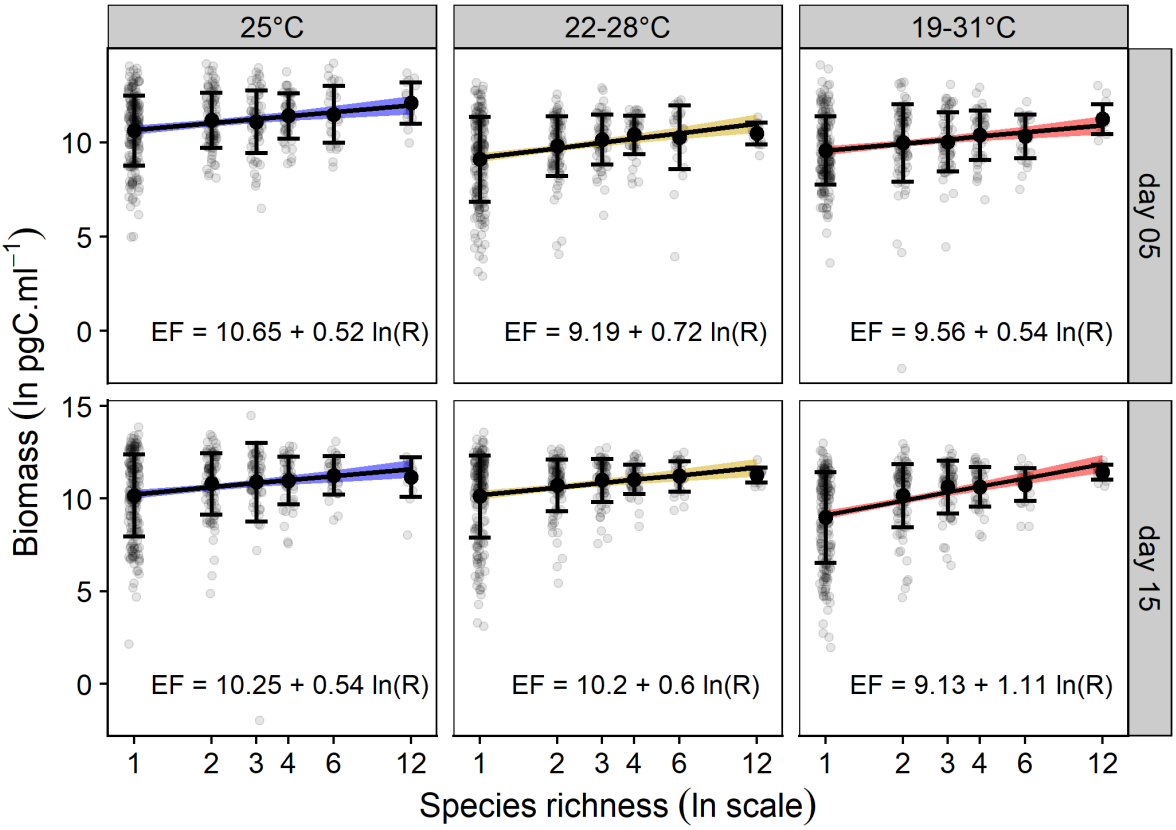

Fig. S1: The relationship between biodiversity and ecosystem functioning measured as biomass depends on the interaction between temperature fluctuation treatment and time.

From left to right: constant 25°C temperature treatment (blue confidence interval), alternating 22 and 28°C temperature every other day (yellow confidence interval), and alternating 19 and 31°C temperature every other day (red confidence interval). Top panel: 5 days, and bottom panel: 15 days of experiment. Grey points represent ecosystem functioning for each of the 1260 communities (420 per temperature fluctuation treatment) measured as ln total cell biomass of Carbon(ln pgC.ml^{-1}). Black points and error bars are the mean ± SD for each level of species richness. Lines and confidence intervals correspond to the fitted curves for the most parsimonious linear mixed model (Table S4). The slope of the relationship between biodiversity and ecosystem functioning depends on the interaction between temperature treatment and time (Table S4), with no differences in slopes between treatments after 5 days but an increase in the slope of the extreme fluctuation treatment over time leading to steeper BEF slopes at high levels of temperature fluctuations at the end of the experiment (Table S5).

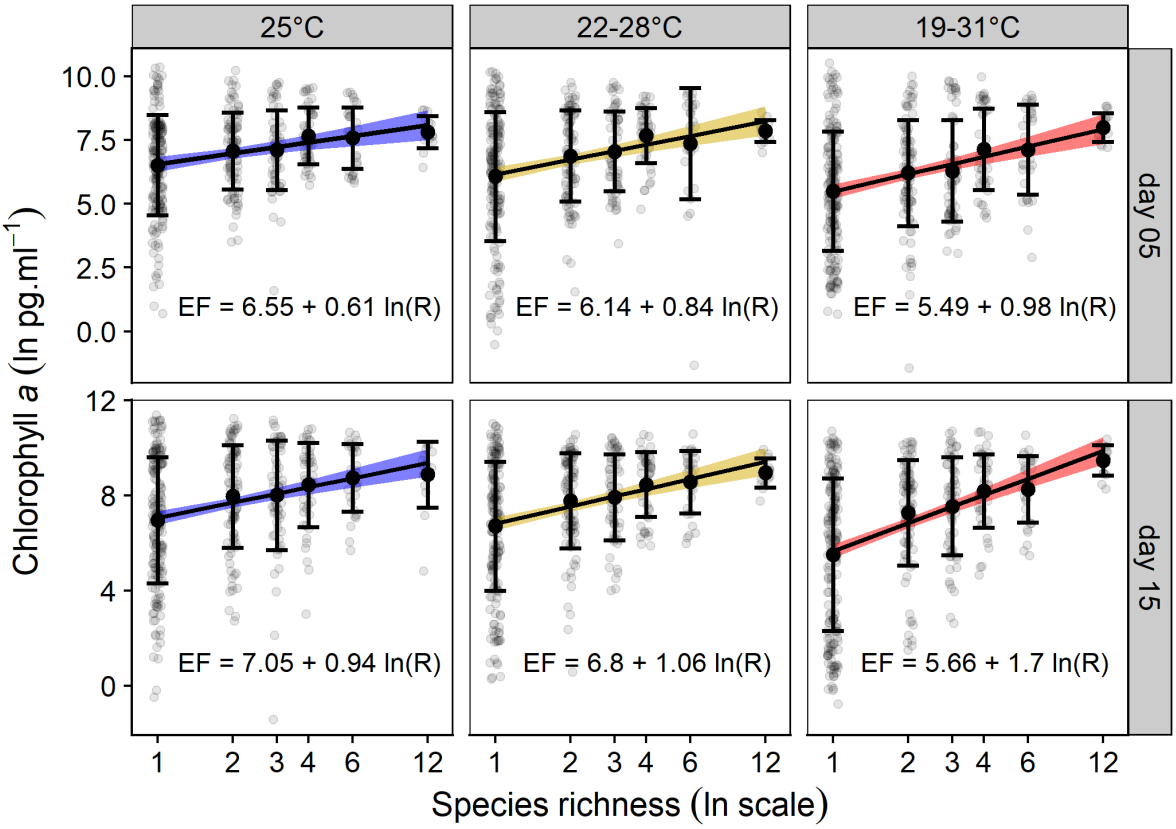

Fig. S2: The relationship between biodiversity and ecosystem functioning measured as chlorophyll *a* depends on the temperature fluctuation treatment and time.

Link between biodiversity and ecosystem functioning measured as total chlorophyll *a* content (ln pg.ml^{-1}) depending temperature fluctuation treatment (from left to right: constant 25°C temperature treatment, alternating 22 and 28°C temperature every other day, and alternating 19 and 31°C temperature every other day) and time (top panel: 5 days and bottom panel: 15 days of experiment). Grey points represent ecosystem functioning for each of the 1260 communities (420 per temperature fluctuation treatment). Black points and error bars are the mean ± SD for each level of species richness. Lines and confidence intervals correspond to the fitted curves for the most parsimonious linear mixed model (Table S6). The slope of the relationship between biodiversity and ecosystem functioning depends on the interaction between temperature treatment and time (Table S6-S7), with no differences in slopes between treatments after 5 days but an increase in the slope at the constant and extreme fluctuation treatment over time leading to steeper BEF slopes at high levels of temperature fluctuations at the end of the experiment (Table S7).

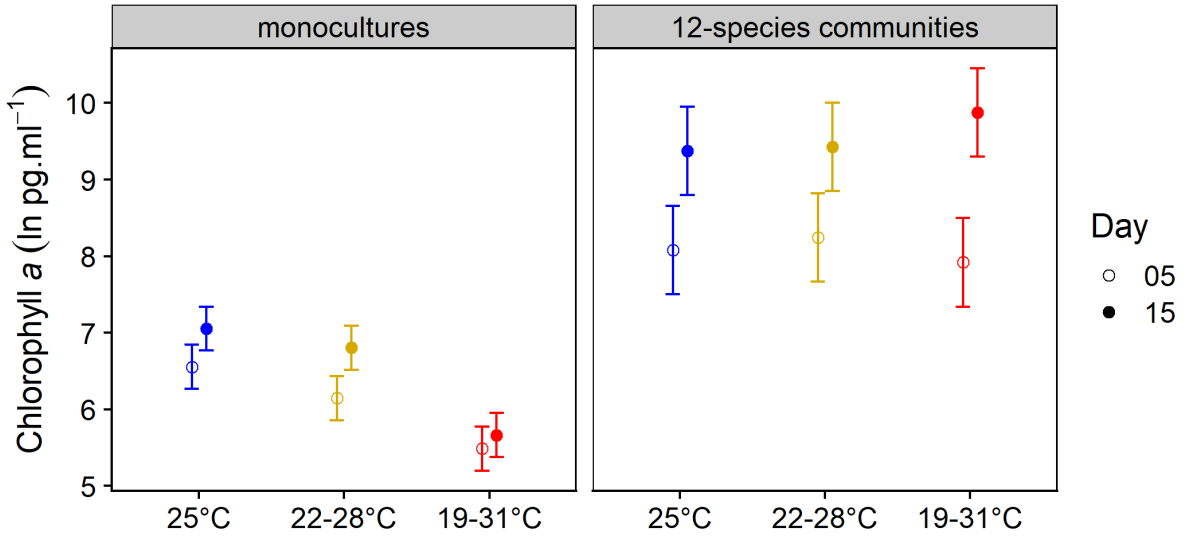

Fig. S3: Comparing ecosystem functioning (as chlorophyll *a*) for the monocultures and 12-species communities in the different temperature fluctuation treatments.

Values of ecosystem functioning (ln chlorophyll *a* pg.ml^{-1}) for the monocultures and 12-species communities in the three temperature fluctuation treatments and the two times (day 5: empty circles, day 15: filled circles). Values and 95% confidence intervals are derived from a contrast analysis of the model represented in Fig. S2 (Table S8). Increased temperature fluctuations lead to lower ecosystem functioning in the low richness communities, while this detrimental effect is compensated for the 12-species rich communities (Table S8). Further, ecosystem functioning increases over time for close to all temperature treatments, but the increase is stronger in 12-species communities than in monocultures (Table S9).

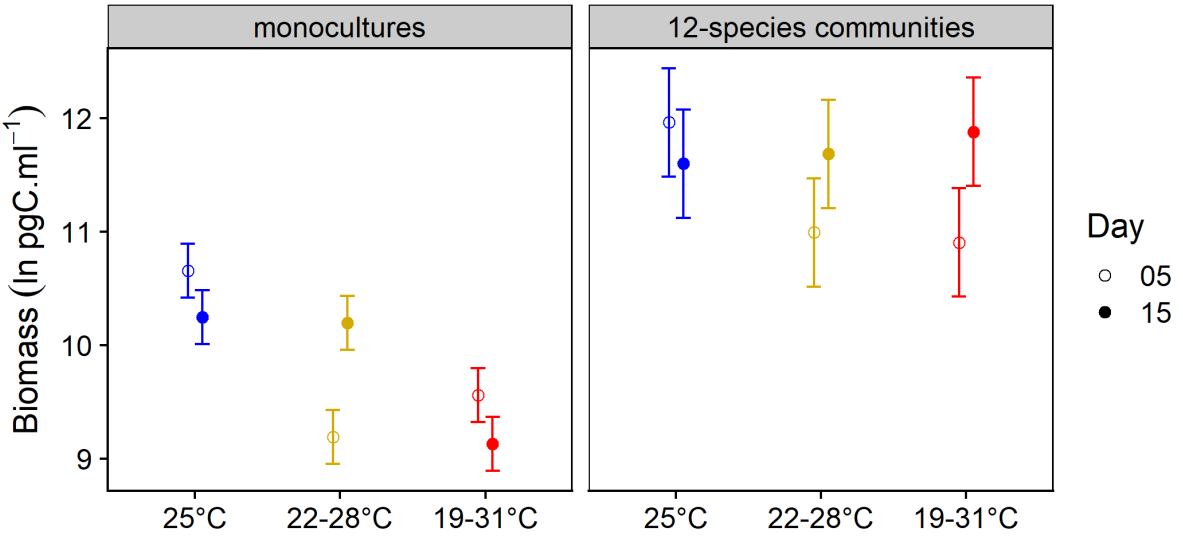

Fig. S4: Comparing ecosystem functioning (as biomass) for the monocultures and 12-species communities in the different temperature fluctuation treatments.

Values of ecosystem functioning (ln biomass of C pg.ml^{-1}) for the monocultures and 12-species communities in the three temperature fluctuation treatments and the two times (day 5: empty circles, day 15: filled circles). Values and 95% confidence intervals are derived from a contrast analysis of the model represented in Fig. S1 (Table S10). Increased temperature fluctuations lead to lower ecosystem functioning in the low richness communities, while this detrimental effect is compensated for the 12-species rich communities at the end of the experiment (Table S10). Further, ecosystem functioning increases over time in the 12-species rich communities particularly in the two fluctuating treatments, while results vary from increases to decreases in the monocultures (Table S11).

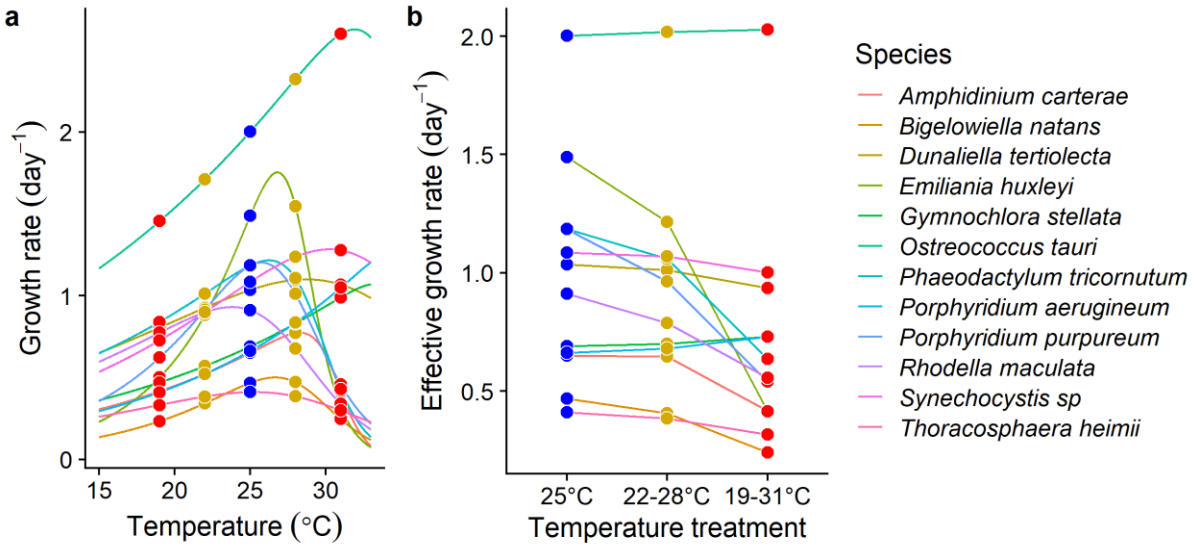

Fig. S5: Extracting effective growth rates from thermal tolerance curves.

a) Thermal tolerance curves are obtained from data from Barton and Yvon-Durocher (1) for all species b) Effective growth rate, representing the tolerance to the temperatures in the experiment, is derived from either the growth at 25°C for the stable treatment (blue dots), or the mean of the growth at 22 and 28°C (yellow dots), or respectively 19 and 31°C (red dots), for the fluctuating treatments. There is a greater spread in effective growth rates (thermal tolerance) among species in the severe fluctuating treatment (relative spread in effective growth rates = 0.80, 0.81 and 0.88, coefficient of variation of effective growth rates = 0.47, 0.49, 0.67 respectively in the 25°C, 22-28°C and 19-31°C treatments). It is interesting to note that much of this increased variation is due to the high tolerance of *Ostreococcus tauri*. Removing this species leads to a relative spread of 0.72, 0.68 and 0.76 and a coefficient of variation of 0.38, 0.34 and 0.41, respectively in the 25°C, 22-28°C and 19-31°C treatments.

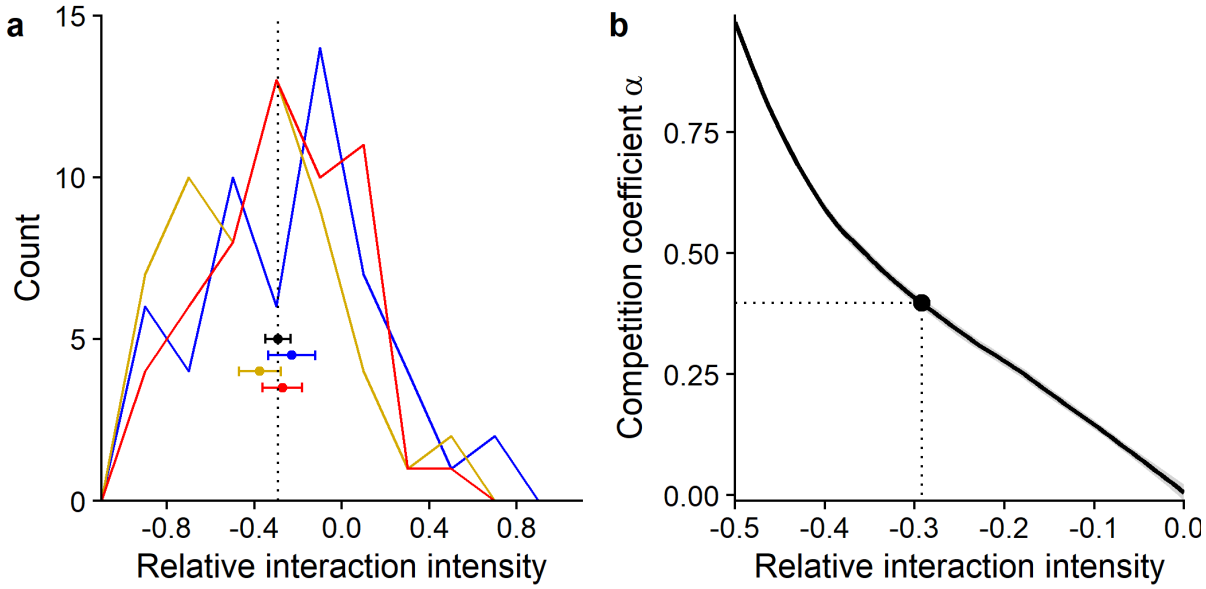

Fig. S6: Distribution of pairwise interaction index measured as relative interaction intensity (9) in the three temperature treatments and relationship between relative interaction intensity and competition coefficient α

a) Relative interaction intensity measured at day 15 for the three temperature treatments (blue: 25°C constant, yellow: 22-28°C fluctuating, red: 19-31°C fluctuating temperature treatments). Frequency polygon with a bin width of 0.2. The points and error bars represent the mean and 95% CI (as 1.96*SEM) of the relative interaction intensity by treatment (colours) and for all treatments pooled (black). Note that not all possible pairwise interactions were investigated, as (1) only the interactions between pairs of species sampled in the random partitioning design were measured and (2) not all pairs of species could be discriminated with the random partitioning design. There is no significant difference in RII between the three temperature treatments (Anova $F_{1,159} = 2.22$, $p = 0.11$) thus we use the mean relative interaction intensity across treatments (in black, RII = -0.29 ± 0.03 SEM, corresponding to the dotted line) to calculate the competition coefficient α. Most of the relative interaction intensities are negative, suggesting competitive interactions where both the effect of species *i* on species *j* and the effect of species *j* on species *i* are negative. But some interactions are positive, representing facilitative interactions. b) Relationship between the competition coefficient α and the relative interaction intensity. Using the theoretical model, we derived RII indices for the pairs of species investigated in the experiment for different α values, using the same thermal tolerances from (1). We then calculate the α value corresponding to the mean experimental RII value from the left panel (dotted vertical line in both panels). The corresponding α value of 0.40 is then used to compare experimental BEF slopes to modelled BEF slopes in Fig. 4.

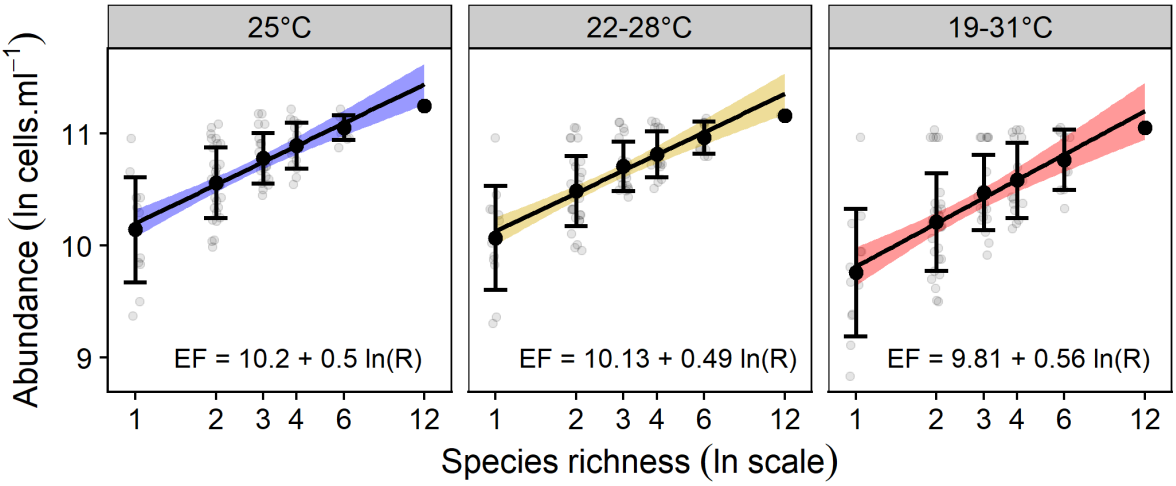

Fig. S7: Modelled relationship between biodiversity and ecosystem functioning at the three temperature levels

From left to right: constant 25°C temperature treatment, alternating 22 and 28°C temperature every other day, and alternating 19 and 31°C temperature every other day. Points represent ecosystem functioning for each of the modelled communities. The competition coefficient corresponds to the competition coefficient measured in the experiment. Abundances values derived from the model are calibrated to the geometric mean of the experimental cells.ml^{-1} values at day 15 in the monocultures at 25°C. Lines correspond to the fitted curves for the most parsimonious linear model. The slope of the relationship between biodiversity and ecosystem functioning depends on the temperature treatment.

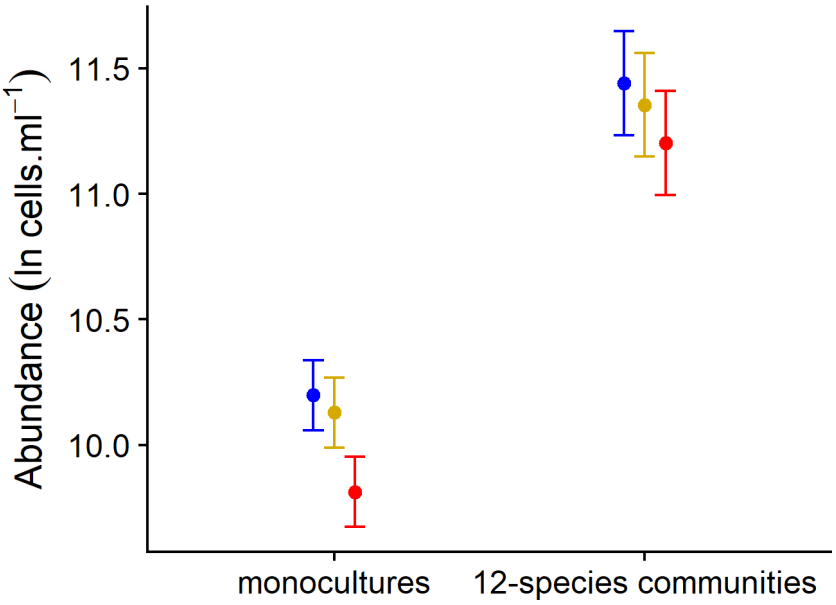

Fig. S8: Comparing theoretical ecosystem functioning at steady state for the monocultures and 12-species communities in the different temperature fluctuation treatments

Values of ecosystem functioning at steady state for the monocultures and 12-species communities in the three temperature fluctuation treatments derived from the theoretical model. Abundances values derived from the model are calibrated to the geometric mean of the experimental cells.ml^{-1} values at day 15 in the monocultures at 25°C. Values and 95% confidence interval are derived from a contrast analysis of the model lm(ln(abundance)~temperature*ln(richness)). Increased temperature fluctuations lead to lower ecosystem functioning in the low richness communities, while this detrimental effect is compensated for the 12-species rich communities.

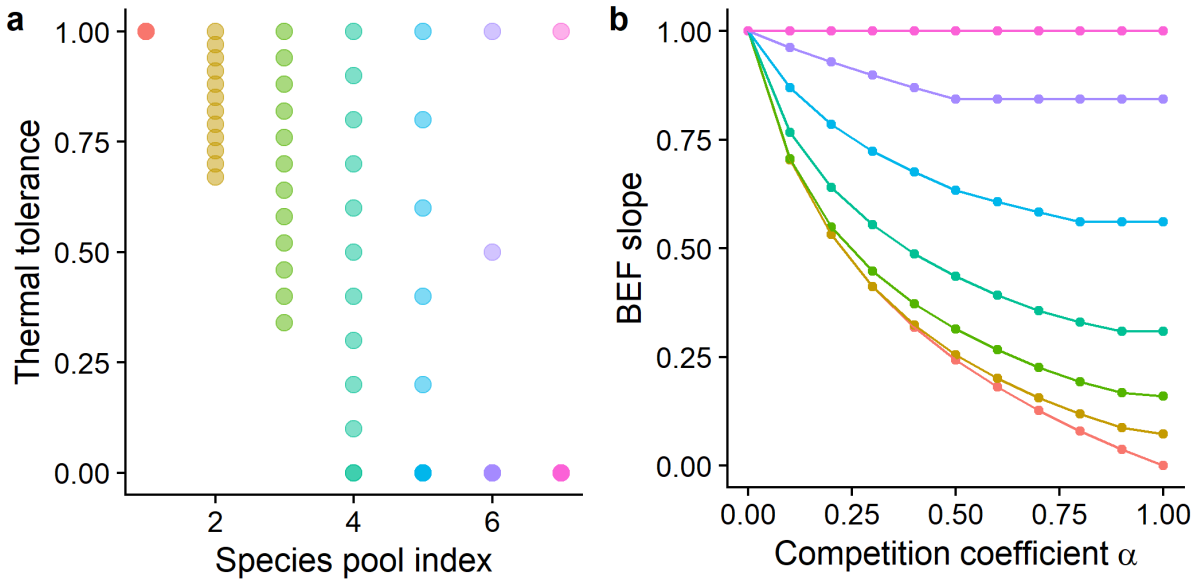

Fig. S9: Dependencies of the biodiversity-ecosystem functioning slopes to the tolerance differences and the competition coefficient

a) Species pools arranged in order of increased tolerance differences. For the red species pool (index 1), tolerance differences are small (i.e. all species have similar growth rate); for the pink species pool (index 7), tolerance differences are large (i.e. one species has a much higher growth rate than the other species). Thermal tolerances are spread equally among species, and all negative values (for higher spreads) are changed to null effective growth rates. Note that we have set the maximum species growth rate equal to one, because this maximum does not affect the BEF slope. b) The BEF slope for the species pools represented in panel a, as a function of the competition coefficient α, i.e. the ratio of interspecific to intraspecific competition a_1/a_0. The BEF slope rapidly declines with increasing competition for a species pool with small tolerances differences (e.g., red species pool), while it is approximately independent of competition strength for a species pool with large tolerances differences (e.g., pink species pool).

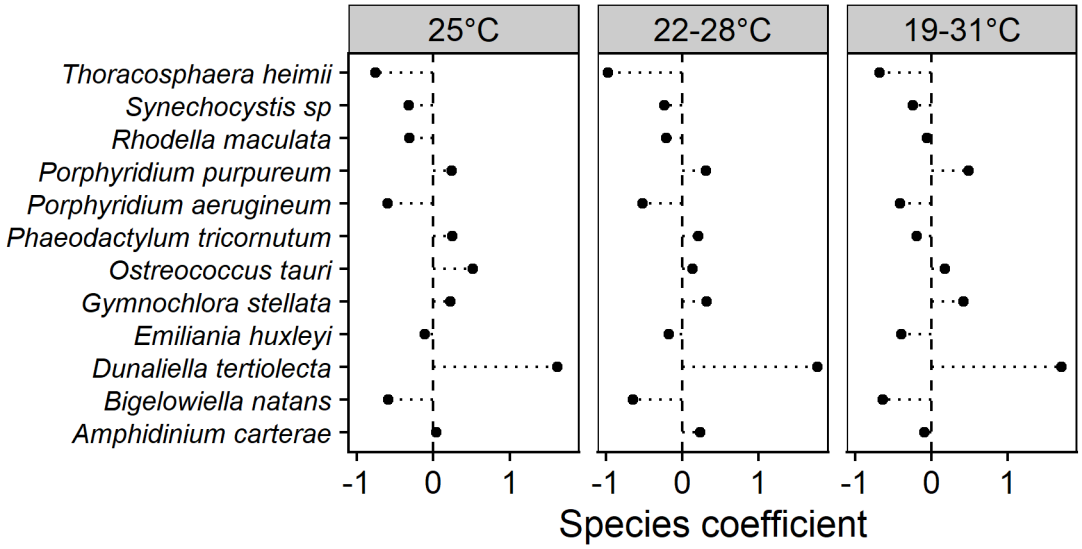

Fig. S10: Species coefficients by temperature fluctuation treatment

Impact of species identity on community functioning after taking into account the impact of species richness. To take into account the impact of species richness, the model uses the residuals of the model 7 presented in Table 1 (lmer(ln(abundance)~ln(R)*T*D+(1|id)) as a dependent variable. The dependent variable is modelled against each of the 12 species modelled as a bivariate presence-absence variable as well as sample identity as a random effect. The model explains 13.6 % of the marginal and 13.7 % of the conditional variance. The figure shows the linear model coefficients for each species at each temperature. Different species have different relative contributions to ecosystem functioning, and these contributions vary with temperature.

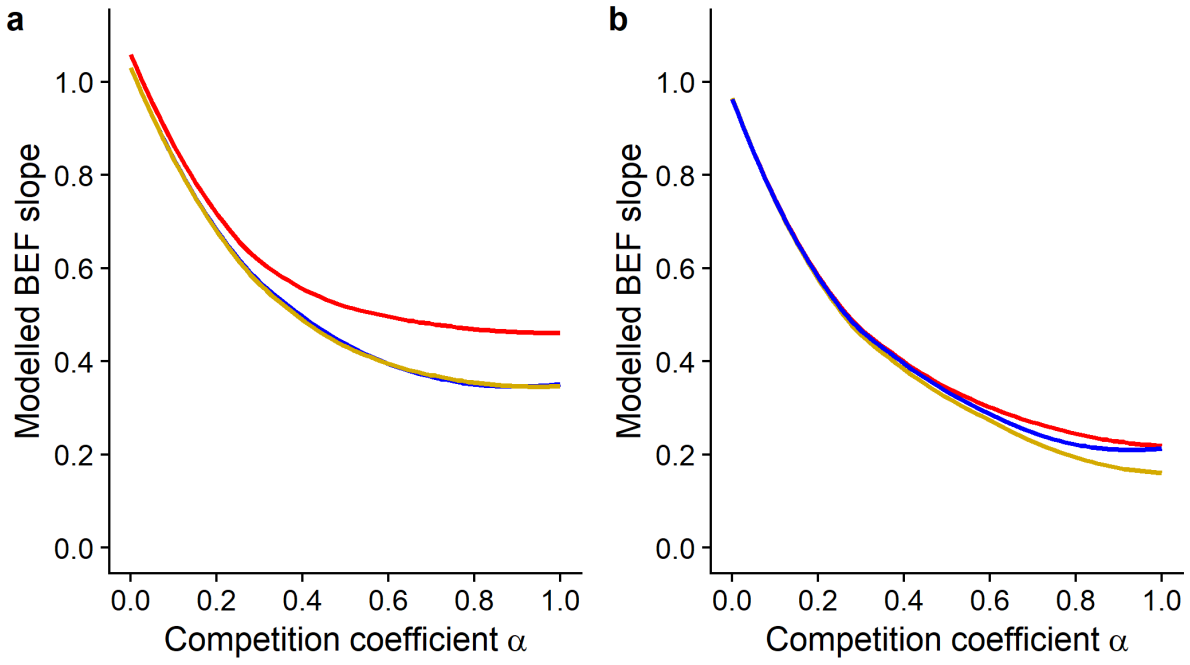

Fig. S11: Modelled biodiversity-ecosystem function slopes either including or excluding *Ostreococcus tauri* from the pool of species

Modelled results show that the spread of species thermal tolerances is important in driving the biodiversity-ecosystem function curve. The higher slope in the 19-31°C treatment is linked to the larger spread in this treatment, however this spread is largely due to the high thermal tolerance of *Ostreococcus tauri* (Fig. S5). We redid the model simulations without this species by sampling species randomly in the pool of 11 species and found a strong decrease in the differences between slopes among treatments, although the 19-31°C treatment still yielded the highest B-EF slope.

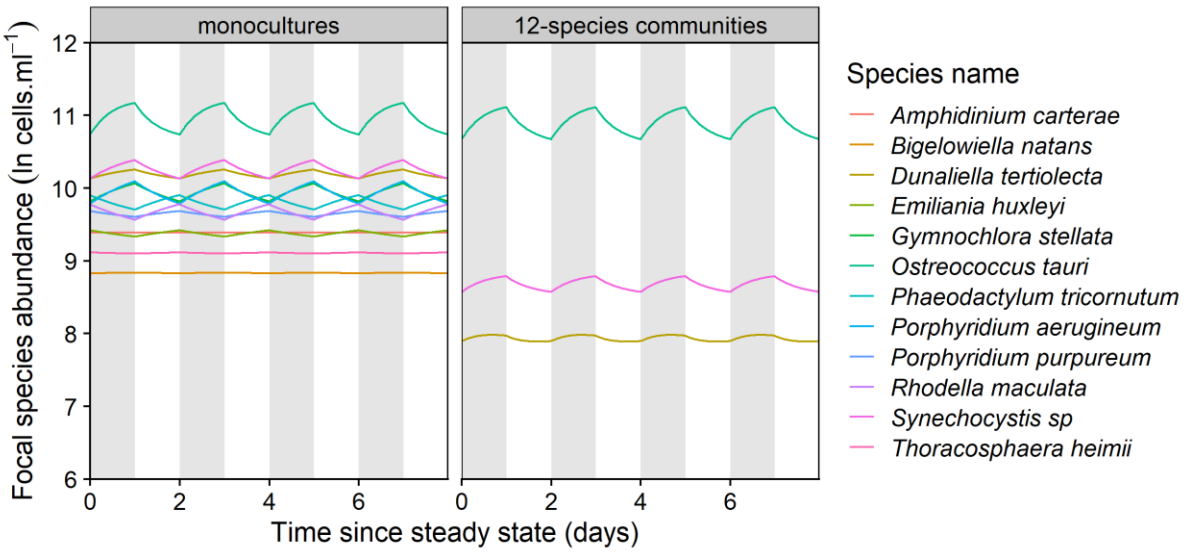

Fig. S12: Modelled fluctuation of species abundances at steady state in monocultures and polyculture in the 19-31°C fluctuation treatment

Modelled species abundances at steady state in monoculture or in the 12-species polyculture. Abundances values derived from the model are calibrated to the geometric mean of the experimental cells.ml^{-1} values at day 15 in the monocultures at 25°C. Because of competitive exclusion, only 3 species persisted in the 12-species polyculture at steady state, they all fluctuate in synchrony. Greyed areas are days where temperature is high. Note that in the monoculture, the most abundant species fluctuate in synchrony, but some species with much lower abundance fluctuate asynchronously (please note that abundance is represented in log scale). However, because these species are competitively excluded in the polyculture, they cannot explain the increased ecosystem functioning in polyculture through temporal insurance effects.

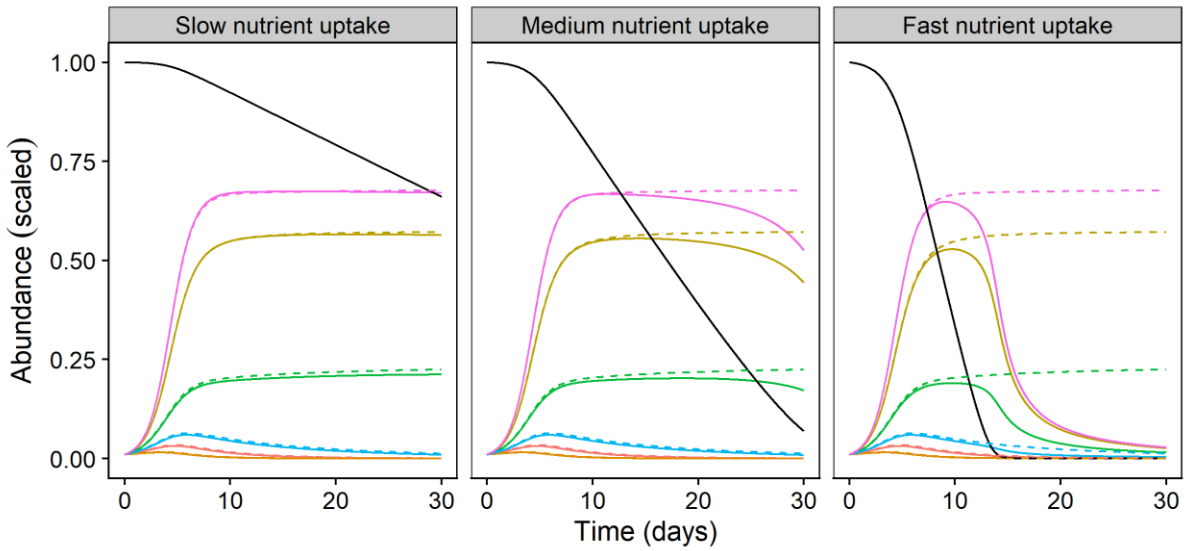

Fig. S13: Effects of nutrient depletion on species abundance dynamics

We compare the trajectories of the simple Lotka-Volterra dynamics and a model in which species abundances are coupled to a nutrient that is continually consumed. Dashed colored lines: species abundances in Lotka-Volterra model; full colored lines: species abundances in coupled model; full black line: nutrient density in coupled model. Model for the 6-species community composed of *Synechocystis sp* (pink lines), *Dunaliella tertiolecta* (yellow lines), *Gymnochlora stellata* (green lines), *Porphyridium purpureum* (blue lines), *Amphidinium carterae* (red lines) and *Bigelowiella natans* (orange lines). Parameter values for the Lotka-Volterra model: growth rates are derived from those measured by Barton and Yvon-Durocher (1) by computing the time-averaged gowth rates in the 19-31°C treatment. Competition strengths a_{ii} = 1 and a_{ij} = 0.4 and initial conditions $N_i(0)$ = 0.01. Parameter values for the coupled model: denoting the growth rate of species *i* by r_i, we set $c_i = 1.06 * r_i$, k_i = 0.03, m_i = 0.03, b_{ii} = 1.0, b_{ij} = 0.4, and $d_i = 0.01 * r_i$ (left panel) or $d_i = 0.03 * r_i$ (middle panel) or $d_i = 0.09 * r_i$ (right panel). Initial conditions $N_i(0)$ = 0.01 and $M_i(0)$ = 1. Thus species growth rates are the same across panels, but nutrient uptake rates ci increase from left to right (compared to left panel, three times faster in middle panel and nine times faster in right panel). From the growth curves measured by Barton and Yvon-Durocher (Fig. S14), it is possible that nutrient uptake is relatively slow in our experiment.

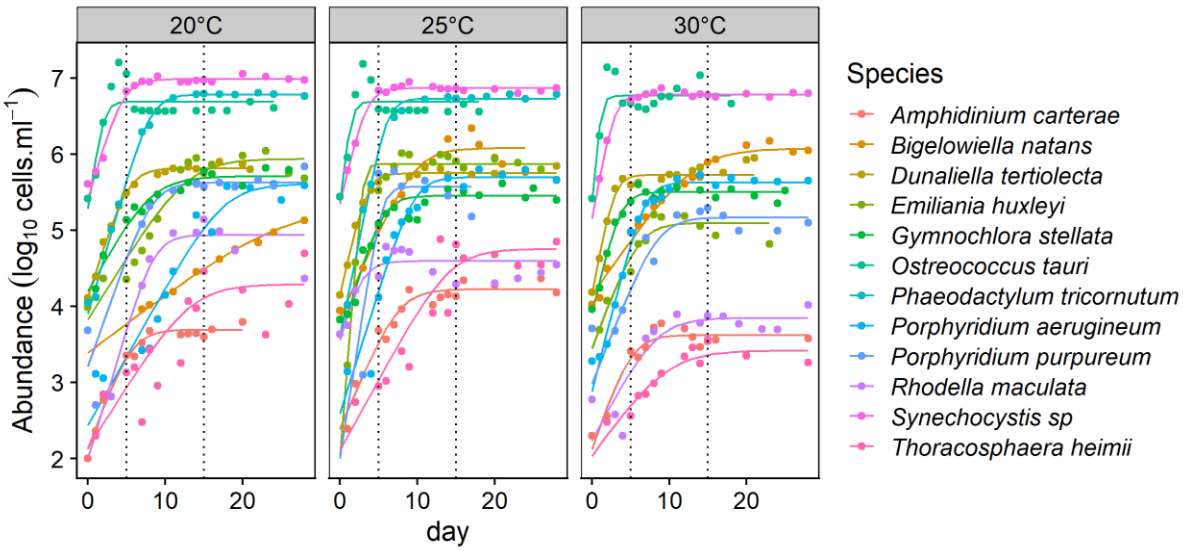

Fig. S14: Growth curves assessed by Barton and Yvon-Durocher (1) at three temperatures

Growth curves are obtained from data from Barton and Yvon-Durocher (1) for all species at three temperatures close to our experimental temperatures, i.e. 20°C, 25°C and 30°C. Note that for *Phaeodactylum tricurnutum*, data was missing at 25°C and 30°C thus we plotted the growth curve at 27°C instead of the curve at 25°C as an approximation. Dotted lines represent the two days of sampling chosen in our experiment, i.e. day 5 and 15. We see that at day 5, most species are still in their exponential phase of growth across all temperatures, but by day 15 most species are in stationary phase. Further, the species stay in stationary phase for up to day 30 with no sign of a drop in abundances, suggesting that nutrients are likely not depleted very fast in our experiment and that modelled steady-state Lotka-Volterra dynamics are a likely good approximation of the true dynamics including nutrient depletion (Fig. S13).

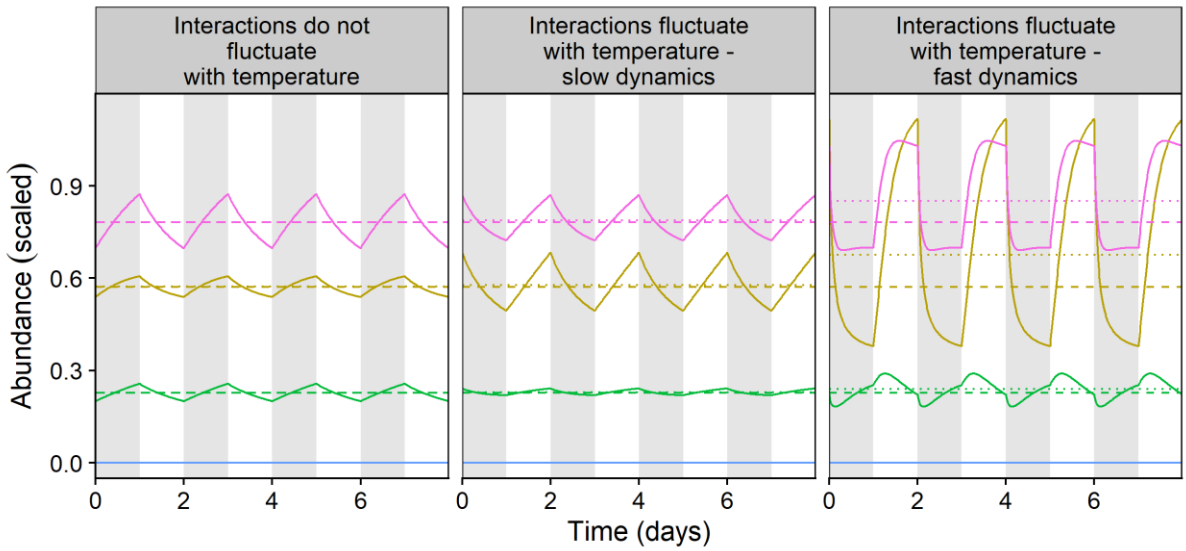

Fig. S15: Time-averaging of the Lotka-Volterra model

We illustrate how well the time-averaged species abundances in steady state can be approximated by the Lotka-Volterra model with time-averaged parameters. a) If the temperature fluctuation does not affect the interactions, the approximation is exact: the time average of the trajectory coincides with the solution of the time-averaged equations (dashed and dotted lines coincide). b) If the interactions fluctuate with temperature, the time-averaged solution (dotted line) and the solution of the time-averaged model (dashed line) differ. If the fluctuations are fast compared to the internal system dynamics, this difference is small. c) If the fluctuations are slower, the difference becomes more important. Model for the 6-species community composed of *Synechocystis sp* (pink lines), *Dunaliella tertiolecta* (yellow lines), *Gymnochlora stellata* (green lines), *Porphyridium purpureum* (blue lines), *Amphidinium carterae* and *Bigelowiella natans* (steady state abundances = 0, hidden below the blue line). Parameter values: growth rates were taken from Barton and Yvon-Durocher (1) at temperatures 19°C and 31°C, denoted by r_i^{low} and r_i^{high} respectively. Competition strength were varied between panels: a) temperature-independent interactions $a_0^{low} = a_0^{high} = 1.0$ and $a_1^{low} = a_1^{high} = 0.4$, b) $a_0^{low} = 0.5$, $a_0^{high} = 1.5$, $a_1^{low} = 0.2$, $a_1^{high} = 0.6$; c) same as panel b, but dynamics are 8-fold accelerated, i.e. growth rates and competition strengths were multiplied by a factor of 8. Trajectories are at steady state, and hence independent of initial conditions. Note that for easier representation, we increased abundance of the most abundant species by 0.1 to avoid overlap with the second most abundant species and better see the differences between dashed and dotted lines for each species. Greyed areas are days where temperature is high.

Table S1: Contrast analysis of the slopes of the biodiversity-ecosystem functioning relationship

Contrast analysis of the slopes of the biodiversity-ecosystem functioning relationship from model 7 in Table 1 (lmer(ln(abundance)~temperature*time*ln(richness)+(1|id)) investigating the slope of the species richness-ecosystem functioning relationship by temperature and time.

Contrast	Subset	Estimate	SE	df	t-ratio	p-value
Between day 5 and day 15						
day 05 – day 15	25°C	0.00	0.09	1,254	0.01	0.989
day 05 – day 15	**22-28°C**	**0.20**	**0.09**	**1,254**	**2.24**	**0.025***
day 05 – day 15	**19-31°C**	**-0.32**	**0.09**	**1,254**	**-3.54**	**<0.001*****
Among the temperature fluctuation treatments						
25°C – 22-28°C	day 05	-0.18	0.13	2,027	-1.38	0.351
25°C – 19-31°C	day 05	0.00	0.13	2,027	0.02	1.000
22-28°C – 19-31°C	day 05	0.18	0.13	2,027	1.40	0.342
25°C – 22-28°C	day 15	0.03	0.13	2,027	0.22	0.975
25°C – 19-31°C	**day 15**	**-0.32**	**0.13**	**2,027**	**-2.53**	**0.031***
22-28°C – 19-31°C	**day 15**	**-0.35**	**0.13**	**2,027**	**-2.75**	**0.017***

Table S2: Contrast analysis of the ecosystem functioning values among temperature fluctuation treatments for a level of species richness of one and twelve

Contrast analysis of the ecosystem functioning at two levels of species richness, either one species or twelve species. The contrast analysis uses model 7 in Table 1, lmer(ln(abundance)~temperature*time*ln(richness)+(1|id)).

Contrast	Time	Estimate	SE	df	t-ratio	p-value
For richness = 1						
25°C – 22-28°C	**day 05**	**0.75**	**0.12**	**2,027**	**6.09**	**<0.001*****
25°C – 19-31°C	**day 05**	**0.63**	**0.12**	**2,027**	**5.12**	**<0.001*****
22-28°C – 19-31°C	day 05	-0.12	0.12	2,027	-0.96	0.600
25°C – 22-28°C	day 15	0.18	0.12	2,027	1.49	0.295
25°C – 19-31°C	**day 15**	**0.99**	**0.12**	**2,027**	**8.04**	**<0.001*****
22-28°C – 19-31°C	**day 15**	**0.81**	**0.12**	**2,027**	**6.55**	**<0.001*****
For richness = 12						
25°C – 22-28°C	day 05	0.31	0.25	2,027	1.26	0.420
25°C – 19-31°C	**day 05**	**0.64**	**0.25**	**2,027**	**2.57**	**0.028***
22-28°C – 19-31°C	day 05	0.32	0.25	2,027	1.31	0.390
25°C – 22-28°C	day 15	0.25	0.25	2,027	1.02	0.566
25°C – 19-31°C	day 15	0.19	0.25	2,027	0.76	0.730
22-28°C – 19-31°C	day 15	-0.06	0.25	2,027	-0.26	0.963

Table S3: Contrast analysis of the ecosystem functioning values between dates for a level of species richness of one and twelve

Contrast analysis of the ecosystem functioning at two levels of species richness, either one species or twelve species. The contrast analysis uses model 7 in Table 1, lm(ln(abundance)~temperature*time*ln(richness)+(1|id)).

Contrast	Temperature	Estimate	SE	df	t-ratio	p-value
For richness = 1						
day 05 – day 15	**25°C**	**0.19**	**0.09**	**1,254**	**2.19**	**0.029***
day 05 – day 15	**22-28°C**	**-0.37**	**0.09**	**1,254**	**-4.23**	**<0.001*****
day 05 – day 15	**19-31°C**	**0.55**	**0.09**	**1,254**	**6.26**	**<0.001*****
For richness = 12						
day 05 – day 15	25°C	0.20	0.18	1,254	1.11	0.269
day 05 – day 15	22-28°C	0.14	0.18	1,254	0.77	0.442
day 05 – day 15	19-31°C	-0.25	0.18	1,254	-1.42	0.154

Table S4: Linear models estimating the effect of temperature fluctuations, species richness and time on ecosystem production measured as biomass.

The linear mixed models describe the effect of temperature fluctuations (T, as a factor), species richness (ln(R)), time (D, days since the start of the experiment, as a factor) and their interaction, plus a random effect of sample identity on ecosystem functioning measured as biomass. At each step, terms are added to the linear model and we compare the two models through a likelihood ratio test. Marginal and conditional R^2 and AIC are calculated for each model, as well as ΔAIC from the model with lowest AIC and AIC weights. Lower AIC values indicate an improved model. Analyses revealed that the model with lowest AIC included the interaction between temperature fluctuations, time and species richness. See Table S5 for a post hoc, multiple comparisons analysis on the slope of the biodiversity-ecosystem functioning relationship by temperature fluctuation treatment and time.

Step	Model	n par	χ^2	df	p-value	R^2m	R^2c	AIC	ΔAIC	AIC weight
0	Intercept+(1|id)	3				0.00	0.50	10,052	306	0.000
1	T+(1|id)	5	70.8	2	4.1e-16	0.04	0.50	9,986	240	0.000
2	T+D+(1|id)	6	8.7	1	3.1e-03	0.04	0.50	9,979	233	0.000
3	T+D+ln(R)+(1|id)	7	111.3	1	5.0e-26	0.10	0.50	9,869	124	0.000
4	T+D+T*ln(R)+(1|id)	9	3.6	2	1.6e-01	0.10	0.50	9,870	124	0.000
5	T+D+T*ln(R)+D*ln(R)+(1|id)	10	3.9	1	4.9e-02	0.11	0.50	9,868	122	0.000
6	T+D+T*ln(R)+D*ln(R)+D*T+(1|id)	12	113.7	2	2.1e-25	0.13	0.55	9,758	12	0.002
7	**T+D+T*ln(R)+D*ln(R)+D*T+D*T*ln(R)+(1|id)**	**14**	**16.4**	**2**	**2.7e-04**	**0.13**	**0.55**	**9,746**	**0**	**0.998**

Table S5: Contrast analysis of the slopes of the biodiversity-ecosystem functioning relationship for biomass

Contrast analysis of the slopes of the biodiversity-ecosystem functioning relationship from model 7 in Table S4 (lmer(ln(biomass)~temperature*time*ln(richness)+(1|id)) investigating the slope of the species richness-ecosystem functioning relationship by temperature and time.

Contrast	Subset	Estimate	SE	df	t-ratio	p-value
Between day 5 and day 15						
day 05 – day 15	25°C	-0.02	0.13	1,254	-0.14	0.885
day 05 – day 15	22-28°C	0.13	0.13	1,254	1.00	0.317
day 05 – day 15	**19-31°C**	**-0.56**	**0.13**	**1,254**	**-4.44**	**<0.001*****
Among the temperature fluctuation treatments						
25°C – 22-28°C	day 05	-0.20	0.18	2,029	-1.13	0.497
25°C – 19-31°C	day 05	-0.02	0.18	2,029	-0.09	0.995
22-28°C – 19-31°C	day 05	0.18	0.18	2,029	1.04	0.554
25°C – 22-28°C	day 15	-0.05	0.18	2,029	-0.31	0.949
25°C – 19-31°C	**day 15**	**-0.56**	**0.18**	**2,029**	**-3.17**	**0.004****
22-28°C – 19-31°C	**day 15**	**-0.51**	**0.18**	**2,029**	**-2.86**	**0.012***

Table S6: Linear models estimating the effect of temperature fluctuations, species richness and time on ecosystem production measured as chlorophyll *a* production

The linear mixed models describe the effect of temperature fluctuations (T, as a factor), species richness (ln(R)), time (D, days since the start of the experiment, as a factor) and their interaction, plus a random effect of sample identity on ecosystem functioning measured as chlorophyll *a*. At each step, terms are added to the linear model and we compare the two models through a likelihood ratio test. Marginal and conditional R^2 and AIC are calculated for each model, as well as ΔAIC from the model with lowest AIC and AIC weights. Lower AIC values indicate an improved model. Analyses revealed that the model with lowest AIC included the interaction between temperature fluctuations, time and species richness. See Table S7 for a post hoc, multiple comparisons analysis on the slope of the biodiversity-ecosystem functioning relationship by temperature fluctuation treatment and time.

Step	Model	n par	χ^2	df	p-value	R^2m	R^2c	AIC	ΔAIC	AIC weight
0	Intercept+(1|id)	3				0.00	0.61	10,852	385.5	0.000
1	T+(1|id)	5	38.2	2	5.2e-09	0.02	0.61	10,818	351.3	0.000
2	T+D+(1|id)	6	165.2	1	8.2e-38	0.05	0.66	10,655	188.1	0.000
3	T+D+ln(R)+(1|id)	7	158.0	1	3.2e-36	0.14	0.66	10,499	32.1	0.000
4	T+D+T*ln(R)+(1|id)	9	9.0	2	1.1e-02	0.14	0.66	10,494	27.2	0.000
5	T+D+T*ln(R)+D*ln(R)+(1|id)	10	28.2	1	1.1e-07	0.15	0.66	10,468	0.9	0.353
6	T+D+T*ln(R)+D*ln(R)+D*T+(1|id)	12	1.2	2	5.6e-01	0.15	0.66	10,470	3.7	0.086
7	**T+D+T*ln(R)+D*ln(R)+D*T+D*T*ln(R)+(1|id)**	**14**	**7.8**	**2**	**2.1e-02**	**0.15**	**0.67**	**10,467**	**0.0**	**0.562**

Table S7: Contrast analysis of the slopes of the biodiversity-ecosystem functioning relationship for chlorophyll *a*

Contrast analysis of the slopes of the biodiversity-ecosystem functioning relationship from model 7 in Table S6 (lmer(ln(chlorophyll a)~temperature*time*ln(richness)+(1|id)) investigating the slope of the species richness-ecosystem functioning relationship by temperature and time.

Contrast	Subset	Estimate	SE	df	t-ratio	p-value
Between day 5 and day 15						
day 05 – day 15	**25°C**	**-0.32**	**0.13**	**1,254**	**-2.38**	**0.017***
day 05 – day 15	22-28°C	-0.21	0.13	1,254	-1.57	0.116
day 05 – day 15	**19-31°C**	**-0.72**	**0.13**	**1,254**	**-5.31**	**<0.001*****
Among the temperature fluctuation treatments						
25°C – 22-28°C	day 05	-0.23	0.21	1,832	-1.07	0.530
25°C – 19-31°C	day 05	-0.37	0.21	1,832	-1.70	0.204
22-28°C – 19-31°C	day 05	-0.14	0.21	1,832	-0.63	0.804
25°C – 22-28°C	day 15	-0.12	0.21	1,832	-0.57	0.838
25°C – 19-31°C	**day 15**	**-0.76**	**0.21**	**1,832**	**-3.54**	**0.001****
22-28°C – 19-31°C	**day 15**	**-0.64**	**0.21**	**1,832**	**-2.97**	**0.008****

Table S8: Contrast analysis of the ecosystem functioning values measured as chlorophyll *a* among temperature fluctuation treatments for a level of species richness of one and twelve

Contrast analysis of the ecosystem functioning measured as total chlorophyll *a* content at two levels of species richness, either one species or twelve species. The contrast analysis uses model 7 in Table S6, lmer(ln(chlorophyll a)~temperature*time*ln(richness)+(1|id)).

Contrast	Time	Estimate	SE	df	t-ratio	p-value
For richness = 1						
25°C – 22-28°C	day 05	0.41	0.21	1,832	1.97	0.121
25°C – 19-31°C	**day 05**	**1.07**	**0.21**	**1,832**	**5.15**	**<0.001*****
22-28°C – 19-31°C	**day 05**	**0.66**	**0.21**	**1,832**	**3.18**	**0.004****
25°C – 22-28°C	day 15	0.25	0.21	1,832	1.20	0.451
25°C – 19-31°C	**day 15**	**1.39**	**0.21**	**1,832**	**6.70**	**<0.001*****
22-28°C – 19-31°C	**day 15**	**1.14**	**0.21**	**1,832**	**5.50**	**<0.001*****
For richness = 12						
25°C – 22-28°C	day 05	-0.17	0.42	1,832	-0.40	0.917
25°C – 19-31°C	day 05	0.16	0.42	1,832	0.38	0.923
22-28°C – 19-31°C	day 05	0.32	0.42	1,832	0.78	0.717
25°C – 22-28°C	day 15	-0.05	0.42	1,832	-0.13	0.991
25°C – 19-31°C	day 15	-0.50	0.42	1,832	-1.20	0.454
22-28°C – 19-31°C	day 15	-0.45	0.42	1,832	-1.07	0.531

Table S9: Contrast analysis of the ecosystem functioning values measured as chlorophyll *a* between dates for a level of species richness of one and twelve

Contrast analysis of the ecosystem functioning measured as total chlorophyll a content at two levels of species richness, either one species or twelve species. The contrast analysis uses model 7 in Table S6, lmer(ln(chlorophyll a)~temperature*time*ln(richness)+(1|id)).

Contrast	Temperature	Estimate	SE	df	t-ratio	p-value
For richness = 1						
day 05 – day 15	**25°C**	**-0.50**	**0.13**	**1,254**	**-3.9**	**<0.001*** **
day 05 – day 15	**22-28°C**	**-0.66**	**0.13**	**1,254**	**-5.1**	**<0.001*** **
day 05 – day 15	19-31°C	-0.18	0.13	1,254	-1.4	0.168
For richness = 12						
day 05 – day 15	**25°C**	**-1.30**	**0.26**	**1,254**	**-5.0**	**<0.001*** **
day 05 – day 15	**22-28°C**	**-1.18**	**0.26**	**1,254**	**-4.5**	**<0.001*** **
day 05 – day 15	**19-31°C**	**-1.96**	**0.26**	**1,254**	**-7.5**	**<0.001*** **

Table S10: Contrast analysis of the ecosystem functioning values among temperature fluctuation treatments for a level of species richness of one and twelve for biomass

Contrast analysis of the ecosystem functioning at two levels of species richness, either one species or twelve species. The contrast analysis uses model 7 in Table S4, lmer(ln(biomass)~temperature*time*ln(richness)+(1|id)).

Contrast	Time	Estimate	SE	df	t-ratio	p-value
For richness = 1						
25°C – 22-28°C	**day 05**	**1.47**	**0.17**	**2,029**	**8.56**	**<0.001*****
25°C – 19-31°C	**day 05**	**1.10**	**0.17**	**2,029**	**6.40**	**<0.001*****
22-28°C – 19-31°C	day 05	-0.37	0.17	2,029	-2.16	0.079.
25°C – 22-28°C	day 15	0.05	0.17	2,029	0.29	0.954
25°C – 19-31°C	**day 15**	**1.12**	**0.17**	**2,029**	**6.51**	**<0.001*****
22-28°C – 19-31°C	**day 15**	**1.07**	**0.17**	**2,029**	**6.22**	**<0.001*****
For richness = 12						
25°C – 22-28°C	**day 05**	**0.97**	**0.34**	**2,029**	**2.81**	**0.014***
25°C – 19-31°C	**day 05**	**1.06**	**0.34**	**2,029**	**3.06**	**0.006****
22-28°C – 19-31°C	day 05	0.09	0.34	2,029	0.25	0.965
25°C – 22-28°C	day 15	-0.09	0.34	2,029	-0.25	0.967
25°C – 19-31°C	day 15	-0.28	0.34	2,029	-0.82	0.692
22-28°C – 19-31°C	day 15	-0.20	0.34	2,029	-0.57	0.836

Table S11: Contrast analysis of the ecosystem functioning values between dates for a level of species richness of one and twelve for biomass

Contrast analysis of the ecosystem functioning at two levels of species richness, either one species or twelve species. The contrast analysis uses model 7 in Table S4, lmer(ln(biomass)~temperature*time*ln(richness)+(1|id)).

Contrast	Temperature	Estimate	SE	df	t-ratio	p-value
For richness = 1						
day 05 – day 15	**25°C**	**0.41**	**0.12**	**1,254**	**3.3**	**<0.001*****
day 05 – day 15	**22-28°C**	**-1.01**	**0.12**	**1,254**	**-8.2**	**<0.001*****
day 05 – day 15	**19-31°C**	**0.43**	**0.12**	**1,254**	**3.5**	**<0.001*****
For richness = 12						
day 05 – day 15	25°C	0.36	0.25	1,254	1.5	0.142
day 05 – day 15	**22-28°C**	**-0.69**	**0.25**	**1,254**	**-2.8**	**0.005****
day 05 – day 15	**19-31°C**	**-0.97**	**0.25**	**1,254**	**-3.9**	**<0.001*****

Table S12: Detailed information about the species

Phyla	Species/Strain	Source location
Chlorophyceae/ Prasinophyceae	*Dunaliella tertiolecta* (CCAP 19/5)	North Atlantic - English Channel
	Ostreococcus tauri (OTH95, RCC 4221)	Mediterranean - Gulf of Lion
Chlorarachniophyceae	*Gymnochlora stellata* (CCMP2057, RCC 626)	West Pacific Ocean
	Bigelowiella natans (CCMP621, RCC 623)	North Atlantic - Sargasso Sea
Rhodophyceae	*Rhodella maculata* (CCAP 1388/2, SAG 45.85)	North Atlantic - English Channel
	Porphyridium purpureum (CCAP 1380/11)	Japan
	Porphyridium aerugineum (RCC 652/ SAG 110.79)	North Atlantic - North Sea
Bacillariophyceae	*Phaeodactylum tricornutum* (CCAP 1052/1B, CCMP 2558)	North Atlantic
Prymnesiophyceae	*Emiliania huxleyi* (CCMP 1516/ CCMP 2090)	South Pacific Ocean
Dinophyceae	*Amphidinium carterae* (CCMP 1314)	North Atlantic - Nantucket Sound
	Thoracosphaera heimi (AC214/ Nap17 /RCC 1512)	Mediterranean - Tyrrhenian Sea
Cyanophycae	*Synechocystis sp* (RCC 1773, R56)	North Atlantic - English Channel